CellPress

Matter

Review

Integration of metal-organic frameworks and covalent organic frameworks: Design, synthesis, and applications

Yang Li,[1,6] Meghdad Karimi,[2,6] Yun-Nan Gong,[3] Nan Dai,[1,4] Vahid Safarifard,[5,*] and Hai-Long Jiang[1,*]

SUMMARY

Metal-organic frameworks (MOFs) and covalent organic frameworks (COFs), featuring porous crystalline materials, have attracted tremendous attention for various applications due to their periodic and well-defined structures, high surface area, and tunable pore architectures. In particular, the facile modification of MOFs and COFs enables their intermesh into MOF/COF hybrids to enhance performance and/or extend scope toward diverse applications. In this review, we provide an overview of significant progress in the design and synthesis of MOF/COF hybrids, including MOF@COF, COF@MOF, MOF + COF, C-MOF, and COF-in-MOF, and their various applications in catalysis, gas adsorption, sensing, energy storage, and photodynamic therapy. The challenges and prospects of the construction of MOF/COF hybrids for various applications are also briefly discussed.

INTRODUCTION

In the past decades, porous materials have captured great attention in physics, chemistry, and materials science. Metal-organic frameworks (MOFs) and covalent organic frameworks (COFs), as crystalline porous materials, have been developed at a very rapid pace.[1,2] MOFs are unique materials because they combine both inorganic and organic components, based on the interaction of coordination bonds between metal ions/clusters and organic linkers.[3–6] On the other hand, COFs are two-dimensional (2D) and three-dimensional (3D) organic frameworks with large structures, which are made entirely of light elements (H, B, C, N, and O) through strong covalent bonds.[7–13] In comparison with the traditional porous materials such as zeolites and activated carbons, MOFs and COFs have unique advantages, including well-defined and tunable structures, large surface area, high porosity, and ease of framework modification, which make them very promising in catalysis, gas sorption and separation, sensing, and drug delivery, among others.[14–29]

The concept of MOFs was developed by Omar M. Yaghi in 1995 and has since advanced rapidly (Figure 1).[2] In the early stage of their development, the focus was mainly on the synthesis of new MOF structures, which was then gradually turned to the study of their performance and applications, especially after the emergence of various stable MOFs (e.g., UiO, MIL, and ZIF).[30–33] Since first being reported in 2005, the development of COFs has continued the development trajectory of MOFs, and has gradually realized the transition from synthesis to applications at present (Figure 1).[8] It is foreseeable that with the continuous, extensive, and in-depth investigations in the application fields, new and higher requirements will be placed on the structural design and synthesis of targeted MOFs and COFs. This requires us on the one hand to develop various elegant new MOF or COF

Progress and potential

The chemistry of metal-organic frameworks (MOFs) and covalent organic frameworks (COFs), collectively referred to as reticular chemistry, has become one of the fastest growing fields of chemistry and materials science. As two important pillars in reticular chemistry, MOFs and COFs have developed in parallel along their respective trajectories for around 2–3 decades, resulting in >80,000 MOFs with >2,000 topologies and >500 COFs with >18 topologies being reported. The integration of structures and functions of these MOFs and COFs will greatly enrich their structures and properties and expand their applications. In addition, the results of integration may also in turn enlighten and promote the development of single MOFs and/or COFs. This review presents an overview of significant progress in the design, synthesis, and applications of MOF/COF hybrid materials. Moreover, the future direction of the nascent field is pointed out.

structures, and on the other hand to integrate the structures and functions of existing MOFs and COFs.[34–36]

In the past two decades, in most cases MOFs and COFs have developed in parallel along their respective trajectories (Figure 1).[32,33] Although we can obtain various MOFs or COFs with different structures by changing variation parameters (e.g., building units, isoreticular expansion, linkages and functionalities, or multivariate [MTV] strategy), the speed of synthesizing new MOF or COF structures with existing methods may become slower due to the difficulties in monomer synthesis and the constraints of linkage types.[32,33] The investigation of integrating MOFs and COFs into one material has begun only in the past several years. Up to now, more than 80,000 MOFs with >2000 topologies and 500 COFs with >18 topologies have been reported (Figure 1).[32,33] The structural and functional integration of these MOFs and COFs will greatly expand their applications, which is conducive to a deeper understanding of structure-activity relationships. The novel structural and functional characteristics brought about by integration may also bring some inspiration to the design of evolutionary structures of MOFs and COFs. For example, classical COFs are linked by strong covalent bonds and generally do not involve open metal sites. Therefore, researchers consciously introduce bipyridine, porphyrin, and phthalocyanine, for example, into the COF skeletons to rivet metal ions for various applications. In contrast, the open metal sites are extensively involved in MOFs and suitable for various catalytic reactions while the strength of the coordination bond in MOFs is usually not strong enough, which restricts their applications under harsh conditions.

However, if we integrate the secondary building units of MOFs into the building units of COFs, the targeted products will present the characteristics of both MOFs and COFs, which not only enlighten the design and synthesis of MOFs and COFs but also enrich their structures and applications.[37] Moreover, the integration can also bring some novel functions that a single component cannot achieve. For example, Li et al. selectively destroyed the coordination bonds in the integrated frameworks based on different strengths between coordination bonds and covalent bonds. The types of defects and their contents can be quantitatively studied by analyzing ^{1}H nuclear magnetic resonance (NMR) spectra of the decomposed products, which is difficult to be realized in the classical COFs and MOFs.[38] In addition, the layered or porous structures of MOFs or COFs are able to provide confined spaces in which to fabricate hierarchical porous materials with special morphologies and sizes that are difficult to be obtained by conventional methods. Ideally, we may be able to realize the uniform distribution of COFs in the pores or adjacent layers of MOFs (Figure 2). The resulting hierarchically porous structures in mesoscopic uniform distribution and related surface interface behavior, as well as their impact on adsorption/desorption, diffusion, and so on, will greatly enrich their applications. Compared with MTV-MOFs and MTV-COFs, the "Heterogeneity within Order" at the mesoscopic scale brings more possibilities for structure and performance regulation (Figure 2). When MOFs in the hierarchical porous materials are selectively etched, COFs with regular morphology can be obtained. For example, Hosono and coworkers report a versatile synthesis of vinyl polymer monosheets with unimolecular thickness by exploiting the 2D nanospaces of MOFs as reaction templates.[39] Theoretically speaking, this method could also be applied in the preparation of 2D COF nanosheets with unimolecularly thick networking architectures, and the thickness of COF nanosheets could be controlled by changing the length of bipyridine in MOF structures.[39]

In general, MOF/COF hybrid materials can be divided into two categories, single component and multicomponent, according to whether they are evenly distributed at the molecular level (Figure 2). Integrating the secondary building units (SBUs) of

[1]Hefei National Laboratory for Physical Sciences at the Microscale, Department of Chemistry, University of Science and Technology of China, Hefei, Anhui 230026, China

[2]Department of Chemistry, Tarbiat Modares University, Tehran, Iran

[3]Key Laboratory of Jiangxi University for Functional Material Chemistry, College of Chemistry & Chemical Engineering, Gannan Normal University, Ganzhou, Jiangxi 341000, China

[4]College of Chemistry and Molecular Engineering, Zhengzhou University, Zhengzhou 450001, China

[5]Department of Chemistry, Iran University of Science and Technology, Tehran 16846-13114, Iran

[6]These authors contributed equally

*Correspondence: vsafarifard@iust.ac.ir (V.S.), jianglab@ustc.edu.cn (H.-L.J.)

https://doi.org/10.1016/j.matt.2021.03.022

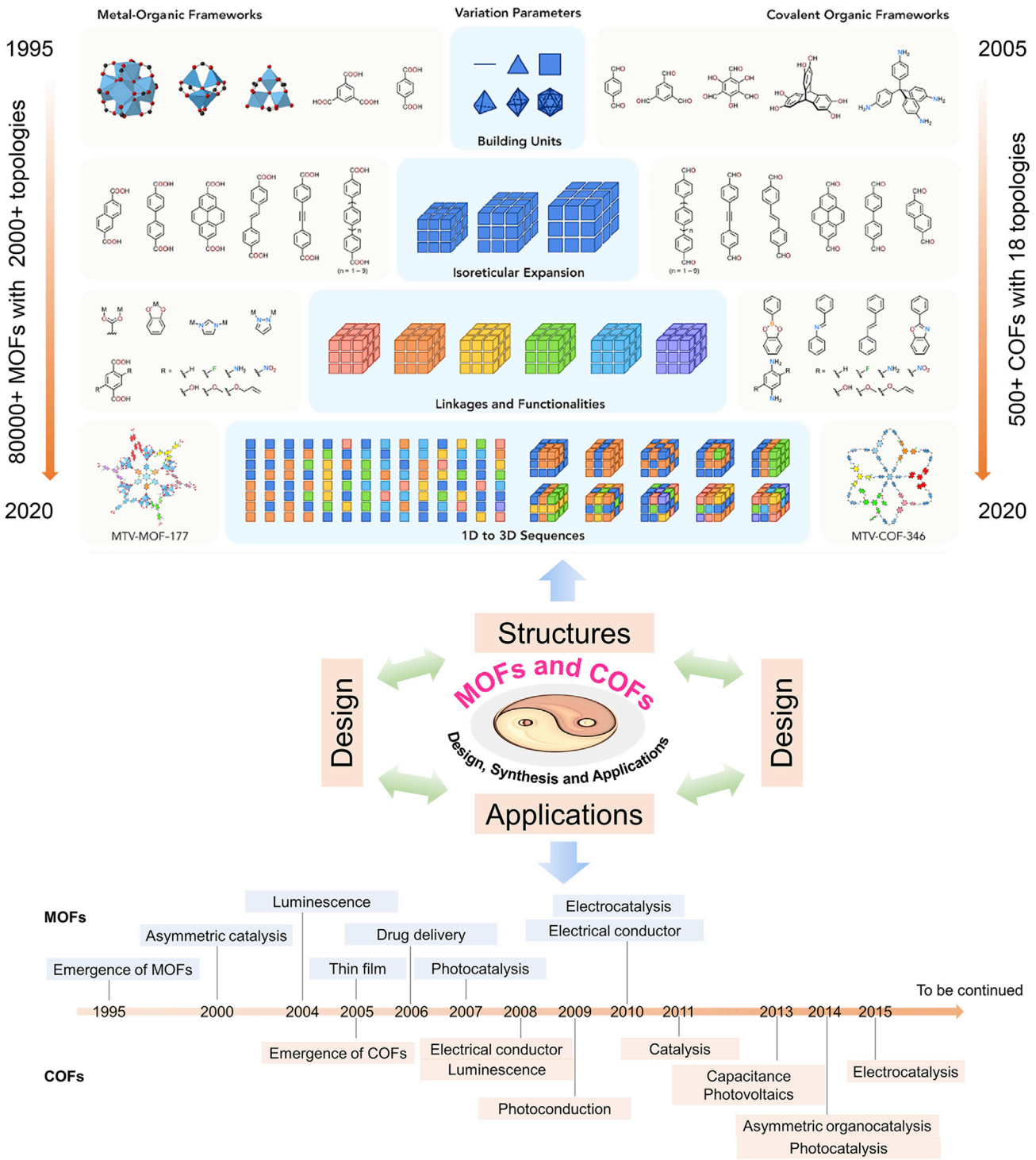

Figure 1. The diversity of MOF and COF structures and the chronology of first reports of applications

The structures and the chronology were adapted with permission from Lyu et al.[33] (Copyright 2020, Elsevier) and Rungtaweevoranit et al.,[1] with permssion (Copyright 2017, Royal Society of Chemistry).

MOFs into the building units of COFs is one of the most common methods for preparing single-component MOF/COF hybrid materials. As shown in Figure 3, three different metal-contained COF linkers, Co-TAPP, $Cu(PDB)_2$, and Cu_3L_3, were chosen

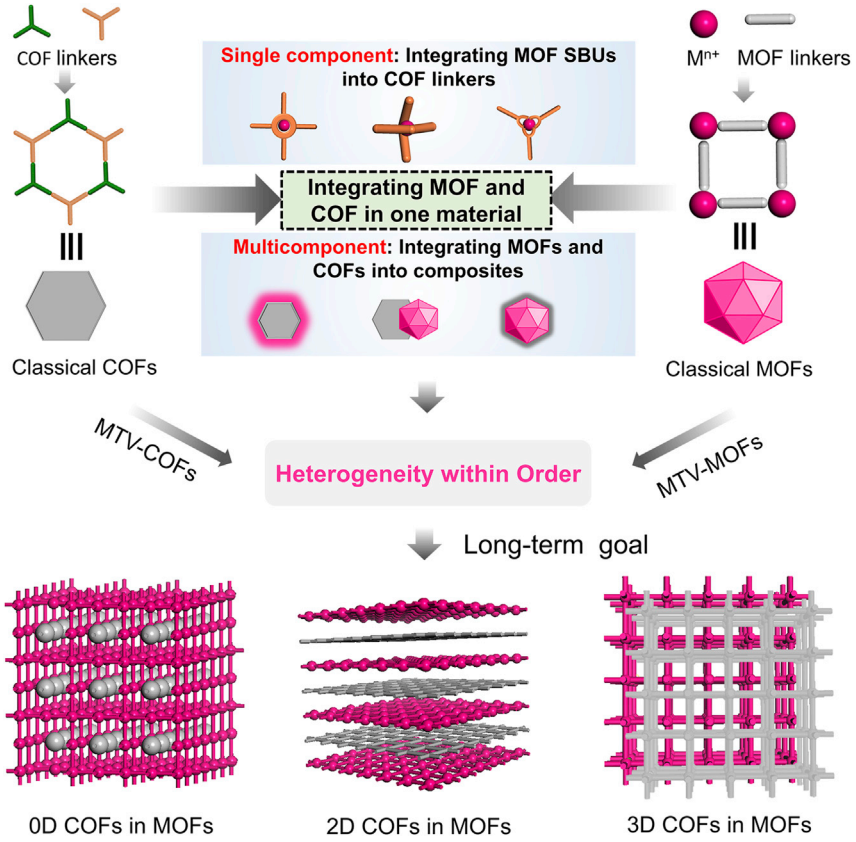

Figure 2. Illustration of MOF/COF hybridizations

to form COF-366-Co,[40] COF-505,[41] and JNM-1,[42] respectively. The metal ions in Co-TAPP do not participate in the formation of C=N linkage and have little effect on the formation of the extended frameworks.[40] By contrast, $Cu(PDB)_2$ in COF-505 helps to assist the direction of the aldehyde and has a greater effect on the formation of the target COF.[41] In JNM-1, the Cu(I) ions are very important: without the Cu(I)

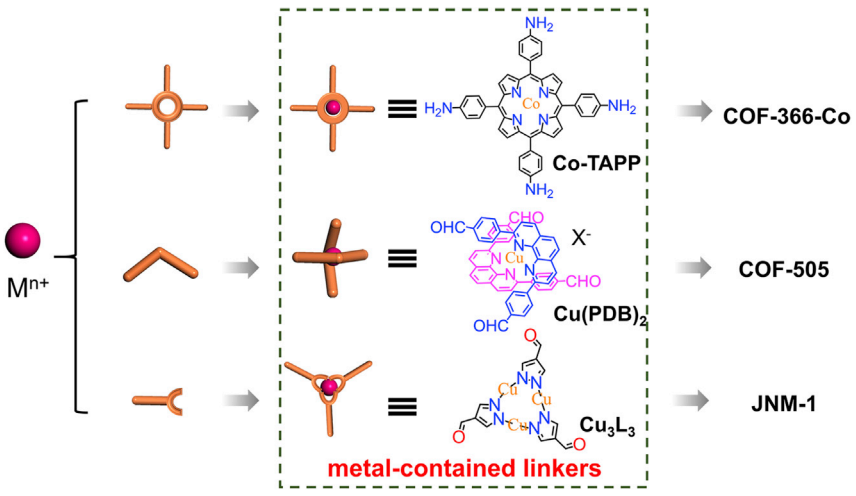

Figure 3. Three reported metal-contained linkers and the related COFs

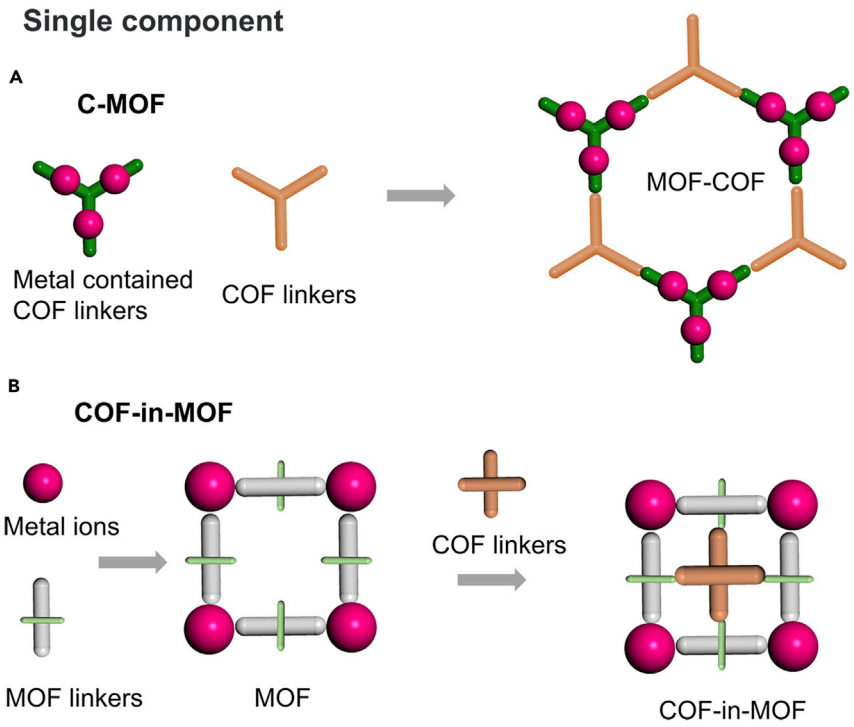

Figure 4. Synthetic strategies for single-component MOF/COF hybrid materials
(A) C-MOF.
(B) COF-in-MOF.

ions, the extended framework structure cannot be formed.[42] JNM-1 can be regarded as a kind of MOF and also a kind of COF. We defined such kinds of single-component MOF/COF hybrids in which all units are in periodic arrangement as C-MOF materials, where C represents covalent (Figure 4A). There is the other special case of single-component MOF/COF, which can be designed and synthesized by employing an as-prepared MOF as a template to grow COFs inside their rigid frameworks. By carefully regulating the size and direction of functional groups in MOFs, we can also obtain single-component MOF/COF hybrids with all units in periodic arrangement, named COF-in-MOF (Figure 4B).

The multicomponent MOF/COF composites are relatively straightforward and easy to understand. Recently, researchers have devoted great efforts to developing various methods to construct multicomponent MOF/COF composites. Fortunately, a large number of MOF/COF composites have been successfully developed, which can be classified mainly on the basis of covalent and non-covalent composite formation, namely MOF@COF, COF@MOF, and MOF + COF (Figure 5). In the first class of composites, COFs are covalently bonded to the surface functional groups of MOFs via covalent bonds to form core-shell structures (Figure 5A), making the composites capable of shell-to-core mass transfer. In the second one, MOFs are grown on the surface of COFs, affording core-shell structures to improve the efficiency of charge separation (Figure 5B). The third one is based on the post-synthetic composite formation approach (Figure 5C). The emergence of these new composites greatly expands the research scope of MOFs and COFs in more application fields.

In pursuit of rational design and development of more creative MOF/COF composites for various applications, we believe it is timely to provide a systematic

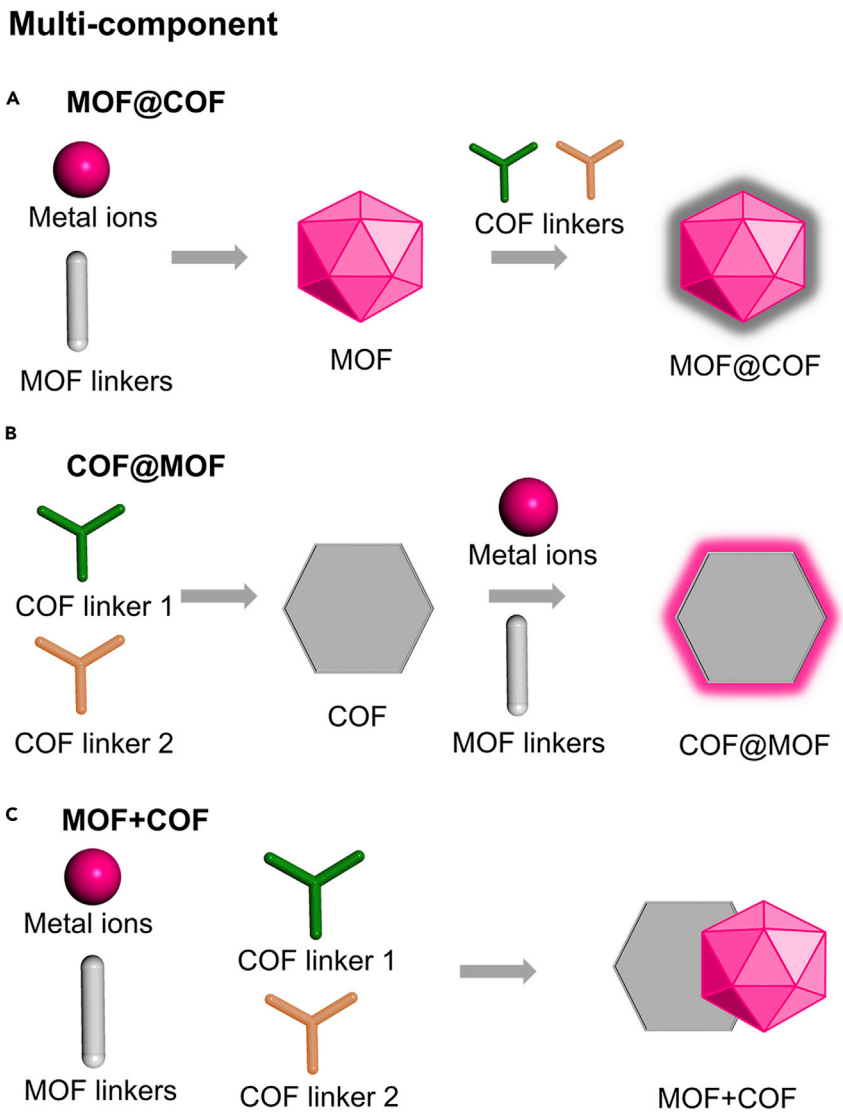

Figure 5. Synthetic strategies for multicomponent MOF/COF hybrid materials
(A) MOF@COF.
(B) COF@MOF.
(C) MOF + COF.

introduction of recent advances in this field. In this review, our discussions start with the design and synthesis of MOF/COF composites, including multicomponent MOF@COF, COF@MOF, and MOF + COF, and single-component C-MOF and COF-in-MOF based on different synthetic protocols. Next, their extensive applications, such as catalysis, gas adsorption, sensing, energy storage, and photodynamic therapy, are introduced. Finally, a summary of the remaining challenges and opportunities in this research field is also critically presented.

SYNTHESIS OF MOF/COF COMPOSITES

Given the diversified compositions and tailorable structures of MOFs and COFs, the MOF/COF hybrid materials have been intensively studied in recent years. Generally, the preparation of MOF/COF composites mainly relies on covalent linkages (e.g., aldimine condensation by amine and aldehyde) or non-covalent linkages (e.g., π-π

stacking interaction) between MOFs and COFs. MOFs as cores generate the shells with COFs by a covalent linking process to form core-shell MOF@COF composites. Given the aromaticity of MOFs and the ordered π-columnar structure characteristics of COFs, strong π-π stacking interaction also provides an opportunity to construct core-shell MOF@COF composites. By covalently binding MOFs onto the surface of COFs, the core-shell COF@MOF composites can be prepared. The fabrication of hierarchical MOF + COF composites with highly dispersed MOF nanoparticles on COF sheets can be achieved by the post-synthetic covalent modification method. The C-MOF and COF-in-MOF coassembly strategies are similar to that of single COFs. These MOF/COF composites not only inherit their merits of high crystallinity, well-defined structures, and large surface area but also provide more possibilities for structural and functional modulation.

MOF@COF

Diverse synthetic methods to construct core-shell MOF@COF composites have been developed. Generally speaking, the core-shell MOF@COF composites were prepared by utilizing MOFs as cores to connect COFs as shells. In recent years, the preparation of MOF@COF composites has been classified into three approaches. The first approach is the construction of amino-functionalized MOFs as cores. COFs are then grown on the surface of MOFs by a covalent linking process to form the MOF@COF composites. Among the reported cases, most studies have been performed using 2-amino-terephthalic acid-based MOFs. For example, Li and coworkers fabricated a new type of MOFs@COFs core-shell composites, where the solvothermal reaction of 2-aminoterephthalic acid and $FeCl_3 \cdot 6H_2O$ led to the formation of the mesoporous NH_2-MIL-101(Fe) MOF as a core.[43] Subsequently, various amounts of 4-formylphenylboronic acid (FPBA) and 1,3,5-tris(4-aminophenyl)-benzene (TAPB) were added to the suspension of NH_2-MIL-101(Fe), whereby the amine-aldehyde condensation reaction between 2-aminoterephthalic acid and FPBA results in covalent binding of FPBA to the surface of NH_2-MIL-101(Fe). Unreacted $-B(OH)_2$ groups of FPBA on the surface of NH_2-MIL-101(Fe) then reacted with free TAPB to form boroxine rings, followed by further amine-aldehyde condensation reaction between TAPB and FPBA leading to the formation of imine groups to generate a series of NH_2-MIL-101(Fe)@NTU-COF composite (MIL@NTU-*x*, with the mass ratio of *x* = 1, 2, 3, 4, or 5) (Figure 6A). The transmission electron microscopy (TEM) images clearly show the core-shell nature of MIL@NTU-*x*. To obtain more direct evidence, energy-dispersive X-ray spectroscopy (EDX) was employed to map the distribution of different elements in MIL@NTU-1, and the results show that the core-shell structured material was formed with a shell thickness of ~6–11 nm. The powder X-ray diffraction (PXRD) patterns of the MOF/COF composites revealed that the thinner the COF shell, the poorer were reflections of NTU-COF while the thicker the shell, the poorer were reflections of NH_2-MIL-101(Fe). Besides, the Fourier transform infrared (FTIR) spectrum of the MOF/COF composites matches well with that of NH_2-MIL-101(Fe) and NTU-COF. Using a similar strategy, the UiO-66-NH_2@COF-TAPB-BTCA composite was constructed by the addition of TAPB and 1,3,5-benzenetricarbaldehyde (BTCA) to the suspension of UiO-66-NH_2. Moreover, a seed growth method to coat MOFs with COFs to form core-shell MOF@COF composites has been also developed by the Wang group.[44] First, a small amount of terephthaldehyde (PDA) and 1,3,5-tris(4-aminophenyl) benzene (PAPB) were added into NH_2-MIL-125 suspension to form heterogeneous seed nuclei, which were grown on the surface of NH_2-MIL-125. Next, an abundant amount of PDA and PAPB was dissolved together in this suspension to obtain highly crystalline NH_2-MIL-125@TAPB-PDA composite (Figure 6B). With the increasing amount of COF shell, the color of the MOF/COF core-shell structures changed gradually from pale yellow

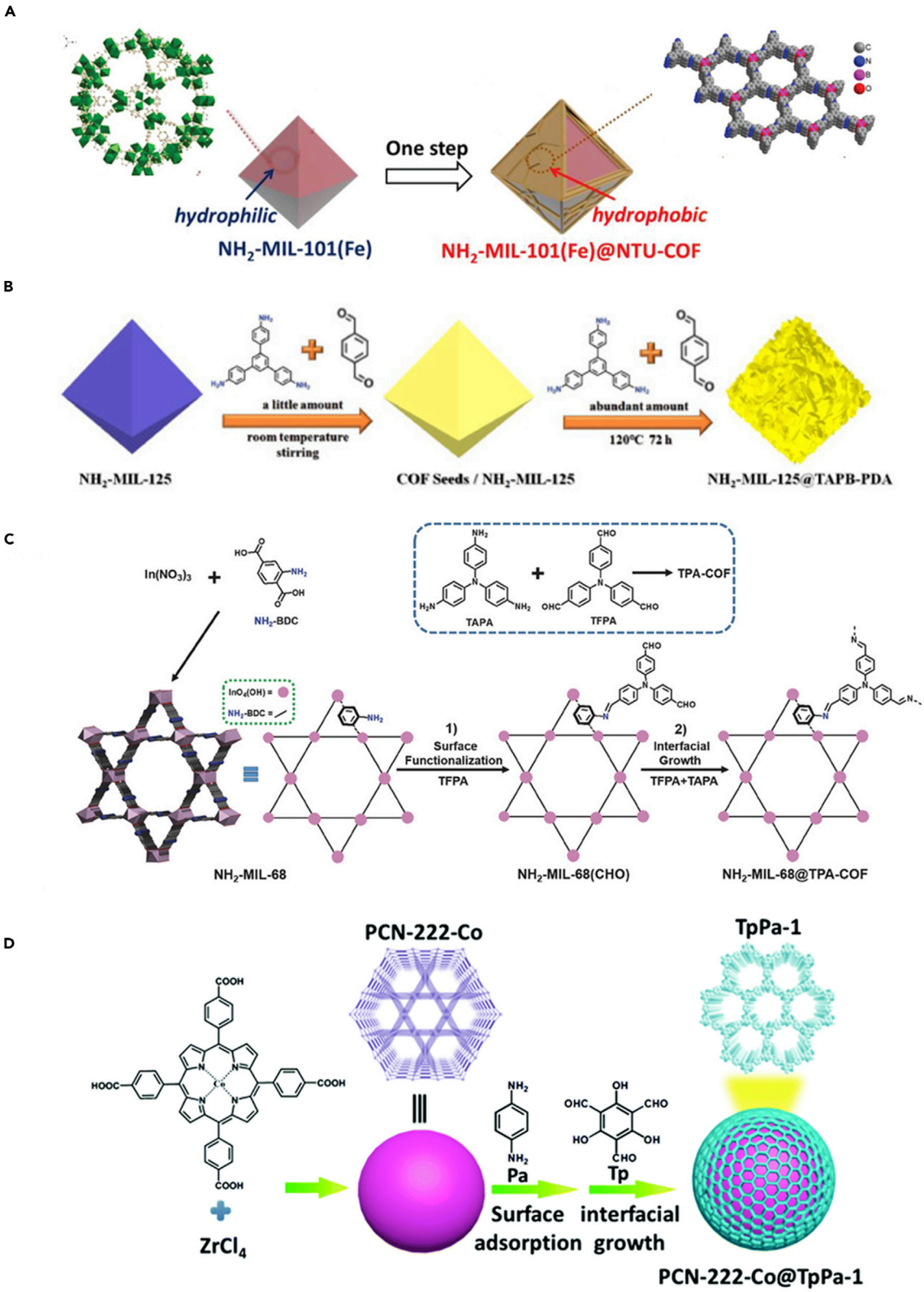
A
One step
hydrophilic
hydrophobic
NH2-MIL-101(Fe)
NH2-MIL-101(Fe)@NTU-COF
B
a little amount
room temperature stirring
abundant amount
120°C 72 h
NH2-MIL-125
COF Seeds / NH2-MIL-125
NH2-MIL-125@TAPB-PDA
C
In(NO3)3
NH2-BDC
TAPA
TFPA
TPA-COF
1) Surface Functionalization TFPA
2) Interfacial Growth TFPA+TAPA
NH2-MIL-68
NH2-MIL-68(CHO)
NH2-MIL-68@TPA-COF
D
PCN-222-Co
TpPa-1
ZrCl4
Pa
Tp
Surface interfacial adsorption growth
PCN-222-Co@TpPa-1

Figure 6. Schematic illustrations of the synthesis of composites
(A) NH_2-MIL-101(Fe)@NTU-COF. From Cai et al.,[43] with permission. Copyright 2019, Wiley.
(B) NH_2-MIL-125@TAPB-PDA hybrids. From Lu et al.,[44] with permission. Copyright 2019, Elsevier.
(C) NH_2-MIL-68@TPA-COF. From Peng et al.,[45] with permission. Copyright 2017, Wiley.
(D) PCN-222-Co@TpPa-1. From Gao et al.,[46] with permission. Copyright 2019, Royal Society of Chemistry.

to bright yellow, which is beneficial to optical absorption in the visible region. The PXRD spectra of the core-shell NH_2-MIL-125@TAPB-PDA composites show that the skeleton structures of NH_2-MIL-125 can be well maintained after integrating with COF. Compared with the FTIR spectra of pure MOF and the core-shell composites, we can find a new peak at a wavenumber of 1,700 cm^{-1}, indicating the successful formation of core-shell composites by Schiff-base condensation reaction.[44]

The second approach is the preparation of aldehyde-functionalized MOFs that serve as cores followed by a two-step method to form core-shell MOF@COF composites. First, the reaction of aldehyde-based building units with amino-functionalized MOFs forms aldehyde-functionalized MOFs(CHO). The COFs are then constructed on the surface of MOFs(CHO) by amine-aldehyde condensation reaction to form MOF@COF composites. Zhang and coworkers employed NH_2-MIL-68 to act as a core, which was functionalized with tris(4-formylphenyl)amine (TFPA) to form aldehyde-functionalized NH_2-MIL-68 (defined as NH_2-MIL-68(CHO)). The solvothermal reaction of NH_2-MIL-68(CHO), TFPA, and tris(4-aminophenyl)amine (TAPA) then results in the NH_2-MIL-68@TPA-COF composite (Figure 6C).[45] As can be seen in the scanning electron microscopy (SEM) images, the as-synthesized NH_2-MIL-68 has a rod-like morphology. The morphology and crystalline structures can be maintained after the surface functionalization of NH_2-MIL-68 with TFPA to form NH_2-MIL-68(CHO). From the FTIR spectrum of NH_2-MIL-68(CHO), a typical C=O stretching band at 1,694 cm^{-1} can be observed, indicating the successful graft of TFPA on the surface of NH_2-MIL-68. The successful preparation of NH_2-MIL-68@TPA-COF core-shell composites was confirmed by FTIR, SEM, and XRD. The FTIR spectrum of NH_2-MIL-68@TPA-COF matches well with that of NH_2-MIL-68 and TPA-COF, indicating the formation of core-shell composites. The crystalline TPA-COF coated on NH_2-MIL-68 has a sheet-like morphology with a thickness of 50–200 nm.[45] With this in mind, Zhao's group synthesized UiO-66-NH_2@COF-TpPa by allowing amino groups in UiO-66-NH_2 to react with aldehyde groups in 1,3,5-triformylphloroglucinol (Tp), followed by reaction with *p*-phenylenediamine (Pa).[47] Moreover, a variety of novel La^{3+}-,Sb^{3+}-doped MOF-In_2S_3@FcDc-TAPT COF composites reported by He et al. have been prepared with NH_2-MIL-68(In) as a matrix. The surface of La^{3+}-,Sb^{3+}-doped MOF-In_2S_3 many amino groups, which were subjected to an aldehyde condensation reaction with ferrocene-1,1′-dicarbaldehyde (FcDc) to form aldehyde-modified MOF, followed by the condensation of a large number of FcDc and 2,4,6-tris(4-aminophenyl)-1,3,5-triazine (TAPT), La^{3+}-,Sb^{3+}-doped MOF-In_2S_3@FcDc-TAPT composites were generated.[48] SEM images show that NH_2-MIL-68(In) has a uniform rod-like structure with length of 2–3 μm. When the MOFs and COFs materials are hybridized, the size of the rod-like composites increases. TEM images show that thickness of the COF coating is 70 nm. The as-prepared MOF@COF composites were also investigated by XRD, X-ray photoelectron spectroscopy (XPS), and FTIR, which also indicated the successful preparation of the target structure.[48]

Based on the above two approaches, the core-shell MOF@COF composites can be constructed by covalent interaction between amino-functionalized MOFs and COFs. In fact, π-π stacking interaction between MOFs without amino or aldehyde groups and COFs can also provide an opportunity to construct MOF@COF composites due to the aromaticity of MOFs and the ordered π-columnar structure characteristics of COFs, which greatly expands the scope of optional MOFs. For instance, Han and coworkers reported

a core-shell MOF@COF composite, which was prepared by using PCN-222-Co as a core. The Pa was uniformly distributed on the PCN-222-Co surface, followed by the interfacial growth of TpPa-1 COF through the reaction of Pa with Tp on the surface of PCN-222-Co, and based on the strong π-π stacking interaction between PCN-222-Co and TpPa-1 to form PCN-222-Co@TpPa-1 composite (Figure 6D).[46] The PXRD pattern of PCN-222-Co@TpPa-1 is in good agreement with the simulated patterns of single MOF and COF. From the FTIR spectra, the appearance of C–N and C=C groups at 1,271 cm^{-1} and 1,584 cm^{-1} also indicated the successful formation of the core-shell composites. The as-prepared MOF/COF hybrids are stable in common solvents, and the structure can still be maintained after soaking in HCl aqueous solution (pH 2) for 24 h. The as-prepared PCN-222-Co has an ellipsoid shape with uniform average size. When coated with TpPa-1, the surface of pristine MOF became rough with the morphology well retained, and the thickness of COF shell could be increased from 3.2 nm to 15 nm. Although this strategy is effective and greatly expands the types of available MOFs, there still exist some shortcomings, such as the serious particle agglomeration or adhesion and incomplete coverage or uneven thickness of COF shells.[46] To solve these problems, Lu and coworkers used polyvinylpyrrolidone (PVP) and branched polyethyleneimine (BPEI) to modify the surface of amino-free UiO-66. PVP can help MOF particles to be uniformly dispersed in the reaction solution, and BPEI can help COF nucleate uniformly on the surface of UiO-66. Under optimized synthetic conditions, a uniform COF layer was grown on the modified seeds to yield well-defined core-shell structures. In contrast, the morphology of the composites without surface modification and with single PVP or BPEI modification was very poor, and the adhesion was serious. In addition, by changing the amount of UiO-66 used in the synthetic conditions, the shell thickness could also be adjusted (Figure 7).[49]

It is worth pointing out that the system for synthesizing MOF@COF is more complicated than that of "pure" COFs, as more effort must be taken to obtain high-crystalline COFs. Up to now, most of the COFs in MOF@COF are linked by C=N linkage. This is mainly due to the good dynamic covalent nature of C=N, which is relatively easier to crystallize on the surface of MOF. To improve the stability of COF shells for applications under harsh conditions, Peng et al. reported the synthesis of MOF@COF followed by aza-Diels-Alder cycloaddition to form aza-MOF@COF. The aza-Diels-Alder reaction between aryl imine and phenylacetylene resulted in the successful conversion of the imine bridges into corresponding quinoline-linked aza-MOF@COF, which can greatly improve the stability of MOF@COF hybrid architectures (Figure 8).[50]

COF@MOF

Recently, the core-shell COF@MOF composites, which were produced by hybridization of COFs and MOFs that serve as cores and shells, respectively, have also received considerable attention. Similar to the synthesis of MOF@COF composites, several synthetic approaches have been developed for the formation of COF@MOF composites. The first approach is one-pot synthetic technology by adding amino-functionalized MOFs into the synthetic reaction system of COFs to form core-shell COF@MOF composites. As a typical example, Lan and coworkers constructed a type of covalently integrated core-shell COF@MOF composite, for which the COF was chosen to construct the composite given its typical structure of Schiff base. First, they prepared NH_2-UiO-66 by heating dimethylformamide (DMF) solution containing $ZrCl_4$ and 2-aminoterephthalic acid. Next, different amounts of NH_2-UiO-66 were added into the reaction system of TpPa-1-COF containing Tp and Pa building units. The slightly extra Tp plays an important role in linking TpPa-1-COF with NH_2-UiO-66 by covalent interaction to form a series of TpPa-1-COF@NH_2-UiO-66 composites with different weight ratios of TpPa-1-COF and NH_2-UiO-66.[51] The PXRD

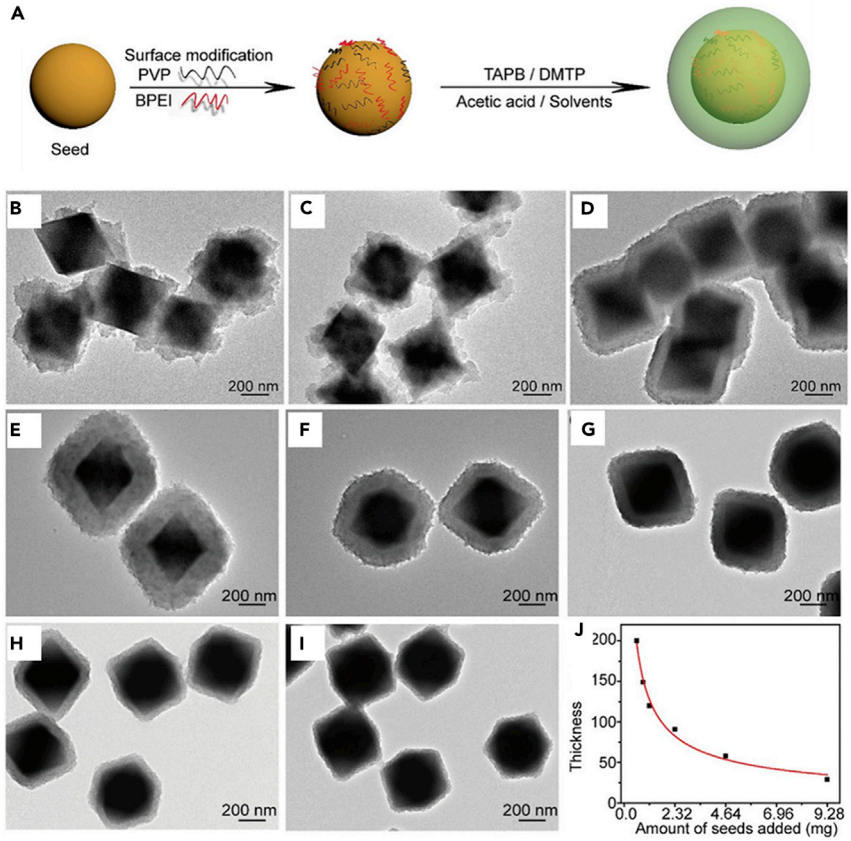

Figure 7. Preparation and characterizations of TAPB-DMTP-COF composites

(A) Schematic illustration of the controlled synthesis of core-shell structured TAPB-DMTP-COF composites.

(B–D) TEM images of TAPB-DMTP-COF composite samples synthesized with (B) unmodified UiO-66 crystal seeds, and those modified with (C) PVP and (D) BPEI.

(E–I) TEM images of TAPB-DMTP-COF composites synthesized with (E) 0.58 mg, (F) 1.16 mg, (G) 2.32 mg, (H) 4.64 mg, and (I) 9.28 mg UiO-66 seeds.

(J) Average thickness of the resulting COF shells versus the amount of MOF seeds used in the synthesis.

From Yao et al.,[49] with permission. Copyright 2019, Elsevier.

patterns of the hybrid materials show good agreement with the corresponding simulated patterns of the single MOFs and COFs, indicating the successful formation of the hybrid materials. The intensity of diffraction peaks of NH_2-UiO-66 apparently increases with the increasing content of the MOFs. The thermostabilities of the resulting COF@MOF hybrids are good and capable of remaining stable under 400°C in air. The permanent porosities of as-prepared COF@MOFs were evaluated by N_2 adsorption and desorption, and all isotherms exhibited type I isotherm. The results show that the Brunauer-Emmett-Teller (BET) surface area of the pure MOF is larger than that of the composites while the BET surface area of the composites is larger than that of the pure COF.[51]

The second approach is the construction of COFs serving as cores, which were then added into the reaction system of MOFs. The organic groups from COF can also coordinate with metal ions of MOF, leading to the growth of MOF on the surface of COF to generate core-shell COF@MOF composite. Sun et al. successfully synthesized imine-based COF by the reaction of 1,4-phenylenediamine and

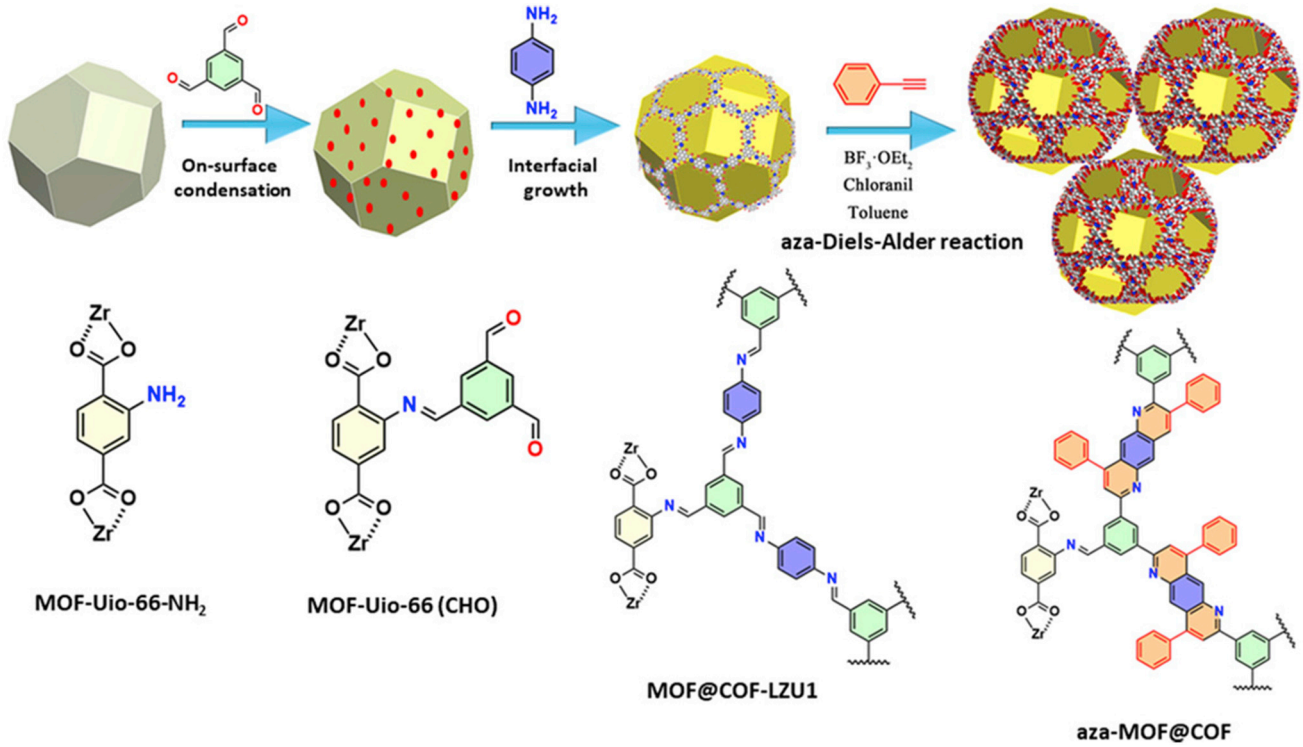

Figure 8. Illustration of the synthetic route of aza-MOF@COF hybrid structure
From Peng et al.,[50] with permission. Copyright 2020, Wiley.

1,3,5-tribenzaldehyde, which was mixed with $Mn(NO_3)_2 \cdot 4H_2O$ and trimesic acid (H_3BTC) in ethanol. It is noteworthy that the Mn^{2+} ions can not only coordinate with H_3BTC to form Mn-MOF but also coordinate with the N atoms of COF. Therefore the COF/Mn-MOF composite was successfully constructed, based on the coordination interaction (Figure 9).[52] It is noteworthy that the integration of Mn-MOF into the pore structure of COF would disturb the periodicity of COF, resulting in poor crystalline form of the resulting COF. The FTIR spectra of the COF/Mn-MOF composites matches well with that of COF and Mn-MOF, and the red-shift of C=N peak in COF@MOF could be ascribed to the coordination effects between the N atoms and Mn centers. Similar conclusions can also be drawn from the Raman spectra and solid-state ^{13}C NMR spectra of COF, Mn-MOF, and COF/Mn-MOF. SEM images show that the morphology of pure COF is a layered-stacking structure with the size of 80–100 nm while that of pure Mn-MOF exhibits as microspheres with the size of ~0.9 μm in diameter. However, for COF/Mn-MOF, the morphology changes to flower-like microspheres with rod-like petals. The distance of the (001) plane in COF is measured as 0.37 nm according to high-resolution TEM (HRTEM) images, which is slightly larger than that of pristine COF (0.35 nm). This could also be ascribed to the introduction of Mn-MOF into the adjacent layers of COF.[52]

Besides the covalent and coordination interactions, the core-shell COF@MOF composites can also be constructed by π-π stacking interaction between COF and MOF. For example, a series of COF@MOF composites were prepared by adding different dosages of COF into the preparation system of MOF, reported by the Zhang group. In this work, the COF was synthesized through the reaction of melamine and cyanuric acid (represented by MCA), which was added into the preparation system of Ce-MOF containing $Ce(NO_3)_3 \cdot 6H_2O$ and 1,3,5-benzenetricarboxylic acid (H_3BTC). By

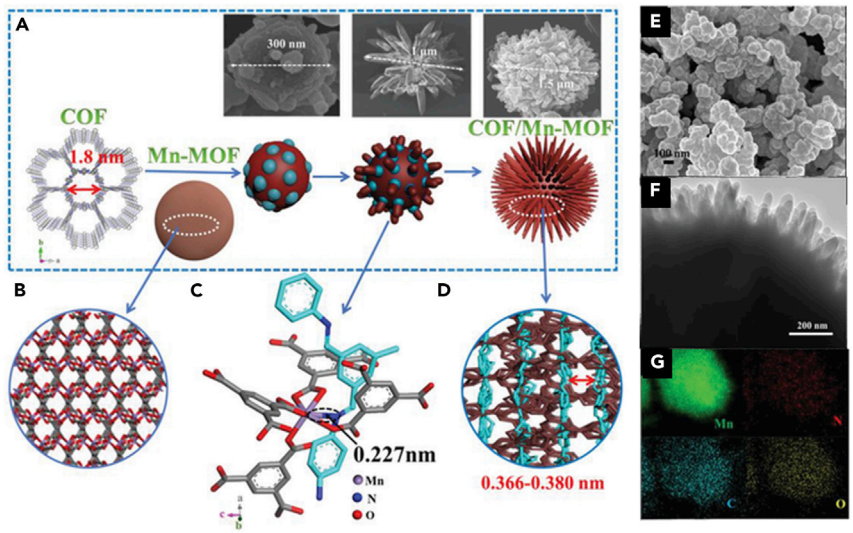

Figure 9. Preparation and characterizations of COF@Mn-MOF hybrids

(A) Schematic diagram showing the growth process of COF@Mn-MOF hybrid, where the inset SEM images indicate the morphology evolution of the COF@Mn-MOF hybrid along with the increased reaction time.

(B) 3D structure of Mn-MOF.

(C) Interlinked COF and Mn-MOF units based on the Mn-N interaction along the *c* direction.

(D) Side view of the COF@Mn-MOF hybrid.

(E) SEM image of COF.

(F) HRTEM image of COF/Mn-MOF.

(G) Elemental mapping images of COF/Mn-MOF.

From Sun et al.,[52] with permission. Copyright 2019, Wiley.

changing the amounts of MCA, a novel MCA@Ce-MOF composite was constructed through π-π stacking interaction between MCA and Ce-MOF. Similarly, they also successfully synthesized another terephthalonitrile (TPN)-COF@Co-MOF composite based on a novel nanoarchitecture of Co-based MOF and terephthalonitrile-based COF, by *in situ* growth of Co-MOF on the TPN-COF surface.[53] The crystal nature and chemical structures of the resulting MOF, COF, and COF@MOF were characterized by PXRD, FTIR, SEM, and TEM. In particular, the XPS characterizations were employed to investigate the chemical components of the obtained frameworks. The core-level XPS spectra of each element were analyzed. The presence of N=C–N and N–C=O indicates the successful formation of MCA through Schiff-base condensation. The fitted C 1s XPS signals of Ce-MOF@MCA composites are composed of MCA as well as Ce-MOF. Moreover, owing to the hybridization of MCA with Ce-MOF, the contents of Ce 3d peaks are lower than that of the pristine Ce-MOF, which is well in accordance with the desired results.[53]

COF@MOF hybrid composites have also been prepared by a modular synthesis strategy. For instance, Zhou and coworkers reported an approach of modular total synthesis to bridge metal and covalent organic frameworks hierarchically in reticular chemistry to form core-shell COF@MOF composites. Firstly, COF-303 single crystals that serve as cores were prepared by an amine-aldehyde condensation reaction between tetratopic aldehyde and phenylenediamine (PDA). The crystals of COF-303 were then immersed in a solution of $Zn(NO_3)_2$ and terephthalic acid (H_2BDC). The MOF-5 was grown on the surface of COF-303 to generate hierarchical COF-303@MOF-5 composite. In this reaction process, the morphology of COF-303 was well maintained due to its excellent stability. COF-303@MOF-5 exhibited a cubic morphology with ordered lamellar surfaces,

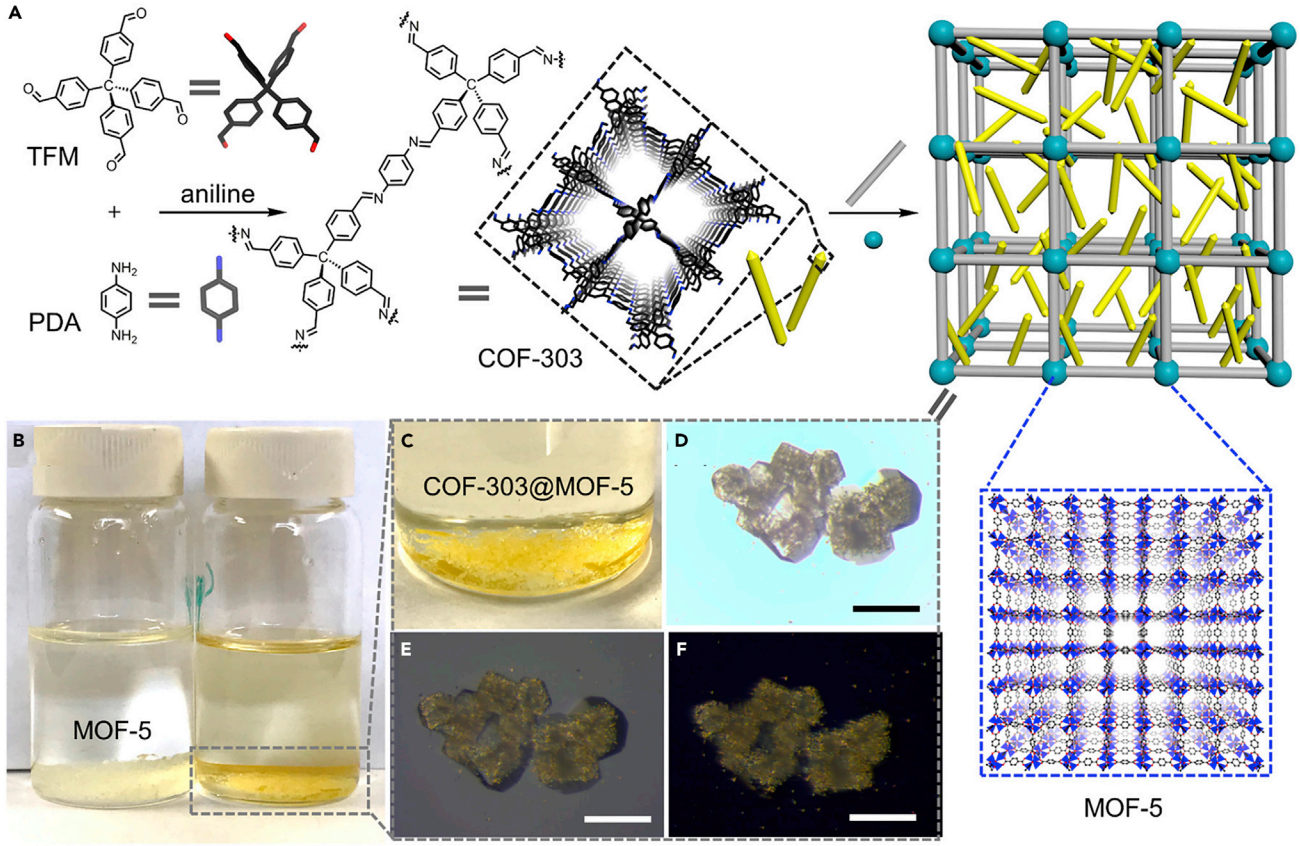

Figure 10. Preparation and characterizations of COF-303@MOF-5

(A) Preparation of COF-303@MOF-5 crystals by stepwise modular synthesis.

(B–F) Optical image of (B) MOF-5 crystals, (C and D) COF-303@MOF-5 crystals, and (E and F) the corresponding polarized optical images placed in between crossed polarizers. Scale bars, 100 μm.

From Feng et al.,[54] with permssion. Copyright 2020, American Chemical Society.

while COF-303 microrods were dispersed on MOF-5, as characterized by SEM. Moreover, the COF-303-to-MOF-5 ratio in the composite could be adjusted by changing the feed ratios of the two modules (Figure 10). A series of other COF@MOF composites such as COF-303@MOF-177, COF-303@MOF-5-Br, COF-303@MOF-5-BPDC, COF-303@ZIF-8, COF-303@UiO-67, COF-303@PCN-160, and COF-300@MOF-5 were also obtained by using the same approach, indicating a general and powerful method to construct hierarchical COF@MOF structures with architectural intricacy.[54]

MOF + COF

Not limited to the formation of core-shell MOF@COF or COF@MOF composites between MOFs and COFs, some other MOF + COF composites without core-shell structures have also been constructed. Very recently, a series of MOF + COF composites were constructed according to different synthesized strategies. The first strategy is the post-synthetic covalent modification of the COFs or MOFs, followed by the introduction of MOFs or COFs on the external surface to form MOF + COF composites. Zou and coworkers used this strategy to prepare one new kind of well-defined and hierarchical MOF + COF composites. First, the polymerization of terephthalonitrile led to the formation of the CTF-1 COF. The amino-functionalized MOFs (NH_2-MIL-125(Ti) and NH_2-UiO-66(Zr)) were also prepared according to the above protocol. The modification of CTF-1 with 4-aminobenzoic acid was then

achieved by a diazo-type reaction process with benzoic acid fragment on the surface of CTF-1. Finally, the dense carboxyl groups of the benzoic acid further reacted with amine groups of MOFs to produce NH_2-MIL-125(Ti)/CTF-1 composites through chemically covalent amide bond interactions. The FTIR spectra show the appearance of a new peak at 1,675 cm^{-1} assignable to amide stretching vibration, while the intensity of C=O peak at 1,722 cm^{-1} from –COOH obviously decreases in the NH_2-MIL-125(Ti) + CTF-1 composite, in sharp contrast to individual CTF-1, indicating that –COOH in B-CTF-1 was converted to an amide group.[55]

The second approach is a one-pot synthetic strategy by adding amino-functionalized MOFs into the reaction system of COF. For instance, Cai et al. reported a series of MOF + COF composites by encapsulating different amine-functionalized MOFs (such as NH_2-MIL-53(Al), NH_2-MIL-125(Ti), and NH_2-UiO-66(Zr)) with a highly stable COF layer (TTB-TTA: a COF synthesized from 4,4′,4″-(1,3,5-triazine-2,4,6-triyl)tribenzaldehyde [TTB] and 4,4′,4″-(1,3,5-triazine-2,4,6-triyl)trianiline [TTA]). In these MOF + COF composites, the amino-functional groups of MOFs were used for covalently linking COF through a convenient condensation reaction, resulting in covalent anchoring of COF onto the surface of MOFs.[56] The chemical composition and crystalline structure of three resulting MOFs was verified by FTIR and PXRD, respectively. The results of ^{13}C solid-state NMR, FTIR, and PXRD for the as-synthesized MOF/COF composites match well with those of TTB-TTA and MOFs. Thermogravimetric analysis revealed that these hybrids are thermally stable under 350°C. The N_2 adsorption isotherms of the three resulting composites showed reversible type IV isotherms, and the BET surface area of NH_2-MIL-53(Al)/TTB-TTA, NH_2-MIL-125(Ti)/TTB-TTA, and NH_2-UiO-66(Zr)/TTB-TTA were calculated to be 322, 1,846 and 1,824 $m^2\ g^{-1}$, respectively, which is higher than those of their parent MOFs.[56]

The MOFs or COFs can also be grown on the COF or MOF membranes to fabricate COF + MOF composite membranes. To achieve this, Ben and coworkers successfully constructed [COF-300] + [Zn_2(bdc)$_2$(dabco)], [COF-300] + [ZIF-8], and [COF-300] + [UiO-66] composite membranes.[57,58] The fabrication procedure of [COF-300] + [Zn_2(bdc)$_2$(dabco)] is as follows. The first stage is the deposition of a layer of polyaniline (PANI) on a SiO_2 disk, followed by the condensation of polyaniline with terephthalaldehyde to form an imine bond for the elimination of water molecules. Next, the reaction of the free aldehyde groups and tetra-(4-anilyl)-methane led to the formation of a defect-free continuous COF membrane, wherein polyaniline not only adheres tightly to the porous SiO_2 but also anchors the COF-300 crystals. Finally, a PANI-modified porous SiO_2 disk comprising COF-300 membrane was added into the synthetic reaction system of [Zn_2(bdc)$_2$(dabco)] containing zinc nitrate hexahydrate, terephthalic acid, and 1,4-diazabicyclo[2.2.2]octane. [Zn_2(bdc)$_2$(dabco)] can be grown on the COF-300 membrane to form [COF-300] + [Zn_2(bdc)$_2$(dabco)] composite membranes by hydrogen bonding between terephthalic acid and the amine group in COF-300.[57] The successful preparation of MOF, COF, and MOF/COF hybrid membranes has been confirmed by SEM. From the cross-sectional SEM images of [COF-300] + [Zn_2(bdc)$_2$(dabco)] composite membrane, the thickness of COF and MOF layer were measured to be ~42 and 55 μm, respectively. The crystallinity of the hybrid membrane was confirmed by PXRD, which showed the expected diffraction peaks of pure MOF, COF, and SiO_2 disk. The fabrication procedure of [COF-300] + [ZIF-8] and [COF-300] + [UiO-66] membranes is similar. Schematic representation of the fabrication of [COF-300] + [UiO-66] composite membranes is shown in Figure 11.[58]

The fascinating features such as high porosity and versatile and tunable pore size promise COFs to be excellent candidates for constructing advanced sieving

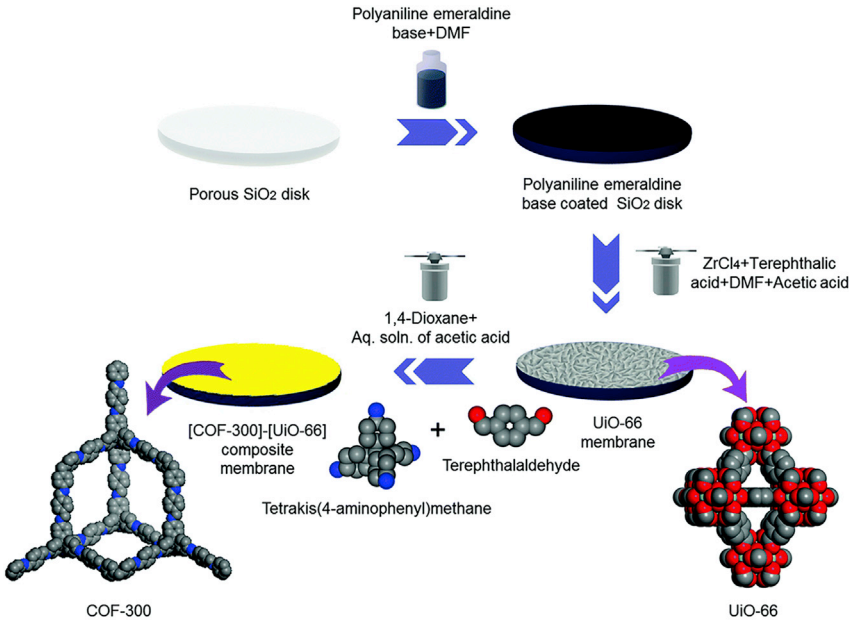

Figure 11. Strategy for the fabrication of the [COF-300]-[UiO-66] composite membrane
From Das and Ben.,[58] with permission. Copyright 2018, Royal Society of Chemistry.

membranes in gas separation. However, limited progress in selective gas separation is achieved due to the pore size of COFs (usually >1 nm) being much larger than the kinetic diameter of common gas molecules (0.25–0.50 nm). To solve this problem, Fan et al. developed a MOF-in-COF concept for the confined growth of MOFs inside a supported COF layer to prepare MOF/COF hybrid membranes.[59] As a proof of concept, two well-established frameworks, ZIF-67 and TpPa-1, were chosen as the building blocks of the target hybrid membrane due to their structural stability. Moreover, the pore size of ZIF-67 is ~0.34 nm, making it attractive in selective gas mixture separation. Structural analysis by XRD revealed that the unit cell the ZIF-67 is smaller than the pore size of TpPa-1, which makes it possible to grow nano-ZIFs inside the confined pores of TpPa-1. Before the preparation of the composite membrane, the COF layer was first grown onto a porous Al_2O_3 substrate, after which the Al_2O_3-supported TpPa-1 membrane was vertically immersed into a cobalt nitrate solution to adsorb Co^{2+} ions. Thereafter, the Co^{2+}-loaded membrane was added to 2-methylimidazole solution to allow the confined growth of ZIF-67, resulting the final MOF/COF hybrid membrane. The thickness of continuous TpPa-1 layer is about 1 μm according to the cross-sectional SEM images, and after the growth of ZIF the color of the as-prepared membranes changed obviously; however, the thickness of the as-prepared membranes remained almost unchanged, the reason for which may be that ZIF-67 might have been grown inside the pores of TpPa-1. EDX revealed that the C and Co signals are uniformly distributed, indicating a good dispersion of ZIF-67 in the pores of TpPa-1. PXRD patterns of TpPa-1 layer and ZIF-67-in-TpPa-1 membrane exhibit a diffraction peak at $2\theta = 4.7^{\circ}$, which can be ascribed to the (100) facet reflection of TpPa-1. However, no obvious ZIF-67 signal was observed in the PXRD pattern of the composite membrane, indicating that ZIF-67 was probably formed inside the TpPa-1 pore rather than as thin layers to cover the COF layer.[59]

C-MOF

The timeline of remarkable progress in the fabrication of C-MOF is shown in Figure 12.[42,60–66] Briefly speaking, the composition of C-MOF is more like that of

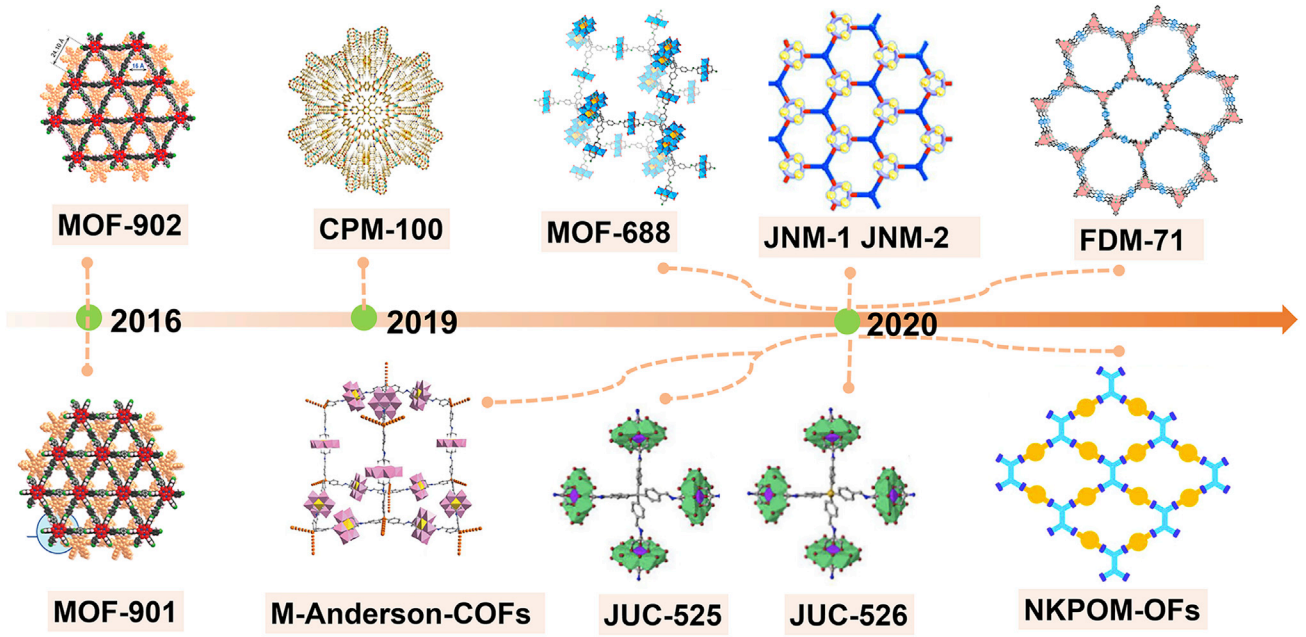

Figure 12. The development of C-MOF
Timeline of remarkable progress made in the fabrication of C-MOFs including MOF-901,[60] MOF-902,[61] CPM-100,[62] M-Anderson-COFs,[64] MOF-688,[63] JUC-525, JUC-527,[65] JNM-1, JNM-2,[42] FDM-71,[38] and NKPOM-OFs.[66]

MOFs while the synthesis condition is more similar to that of COFs. The first C-MOF, named MOF-901, was reported in 2016 by Yaghi and coworkers.[60] MOF-901 was prepared by combining the chemistry of MOFs and COFs. The growth progress of MOF-901 involves *in situ* generation of an amine-functionalized titanium-oxo cluster, which was linked with terephthalaldehyde using an imine condensation reaction. Thus, both covalent and coordination bonds can simultaneously form in a single structure. The structural features of MOF-901 were first examined by FTIR to prove the imine formation, and ^{1}H NMR spectroscopy was employed to gain a better understanding of the cluster composition. The PXRD patterns of MOF-901 were indexed in a primitive hexagonal system with unit cell parameters of $a = b = 27.4037$ and $c = 8.9403$ Å. The SBU of the as-prepared MOF-901 contain a trigonal prismatic Ti_6O_6 inner core, and the Ti atoms in the SBU can be divided evenly over two separate triangular planes and bound to one another through μ_3-O atom. SEM images reveal that the size of MOF-901 is small with no regular shape. Elemental analysis results reveal that the experimental contents of C/N/H in MOF-901 are well in line with the calculated values derived from the proposed structure. This C-MOF represents the first example of combining the chemistry of MOFs and COFs.[60] Later in 2019, Feng and coworkers reported a new pore-space-partition strategy to construct COF-MOF coassembly through one-pot synthesis technology.[62] The metal salts H_2BDC and pyridine-4-boronic acid were dissolved in a mixture of DMF and toluene. During the reaction, the metal ions link with BDC to form MIL-88-type MOFs with open metal sites due to the formation of a 3,9-connected net, in which the metal ions are further coordinated with pyridine-4-boronic acid at the N side. Moreover, the trimer of pyridine-4-boronic acid, named 2,4,6-tri(4-pyridinyl)-1,3,5-boroxine (**tpb**), is formed by the condensation of three boronic acids occurring at the B side with a C_3-symmetric pore-partition. Finally, a COF-MOF coassembly, $[In_{1.2}Co_{1.8}(OH)_{0.8}O_{0.2}(BDC)_3]$tpt, was constructed.[62] In 2020, several C-MOFs were synthesized through imine condensation of Anderson POM-linkers and

4-connected tetrahedral organic aldehyde monomers.[63–66] Polyoxometalates (POMs) are a large family of anionic metal oxide clusters; thus, the skeleton of the POM-containing C-MOF system is negatively charged, which is usually difficult to be realized in pure COFs. These highly crystalline 3D porous crystalline covalent polyoxometalate-organic frameworks exhibited 3-fold interpenetrated diamondoid topology. The selected new POM building units are of critical importance in enriching the structural diversity and expanding the functions of MOF/COF composites.

In addition to the aforementioned examples, Wei et al. reported two sophisticated and reticular C-MOFs by combining the chemistry of Cu(I) clusters and COFs.[36,42] The obtained single-component C-MOF (termed JNM-1 and JNM-2) with cyclic trinuclear units can be synthesized either in a stepwise synthetic approach or in a one-pot reaction (Figure 13). The construction of crystalline, reticular C-MOF by combining metal clusters and organic linkers with covalent bonds is highly challenging and remains scarcely explored, which may be due to the incompatibility of the cluster formation condition with those required for dynamic formation and fracture of covalent bonds. The stability and solubility issues of clusters may also make the synthesis difficult.[42]

It is well known that defects are closely related to the synthesis, characterization, and applications of COFs or MOFs. However, it is still a challenge to accurately describe various types of vacancies with accurate quantification in a framework. It is worth pointing out that, unlike classic COFs and MOFs, C-MOFs contain both the covalent and the coordination bonds. On the basis of the strength difference between coordination bonds and covalent bonds, C-MOF can be digested by dissociating the coordination bonds while keeping the imine linkage intact. Therefore, the types and quantity of defects in the system can be easily studied (Figure 14).[38]

COF-in-MOF

As can be seen in the SEM or TEM images of MOF@COF composites, in most cases MOFs usually play a decisive role in the final morphology of MOF@COF composites.[44,45,49,50,67] Except for growing COFs on the surface of MOFs, one can also grow COFs inside the well-chosen MOFs by taking the latter as template. In this situation, the MOF-templated COFs may inherit the regular morphology and fine crystallinity of the mother MOFs. It may even realize the transformation from MOF single crystals to COF single crystals. MOFs have been used previously for template synthesis of polymer using flexible crosslinkers. Although the morphology can be well maintained, no crystalline polymer structures can be obtained due to the flexibility of the crosslinkers.[68] The linkers of COFs are relatively rigid, and it is experimentally extremely challenging to grow extended COF frameworks as the distances, angles, and arbitrary rotations of the linkers in MOFs should match optimally with each other. Thus no experimental results were reported so far that combine the topological variability of MOFs with the fascinating features of COFs to form COF-in-MOF materials. Recently, Ahmad et al. reported an effective geometric method to develop an ideal MOF crosslinker pair by employing a high-throughput screening approach. For a given crosslinker, the presented screening method contains (1) candidate selection, (2) rotation, (3) angle check, (4) distance check, and (5) combining suitable MOF candidates with the given crosslinker for molecular dynamics simulations to optimize the structure.[69]

Six commercially available crosslinkers (CL1–CL6) were screened to look for novel structures and prime candidates for future COF-in-MOF. Some of the results are shown in Figure 15. The reported approach provides an optional path for the design and synthesis of novel and fascinating COF-in-MOF materials as well as other related structures.[69]

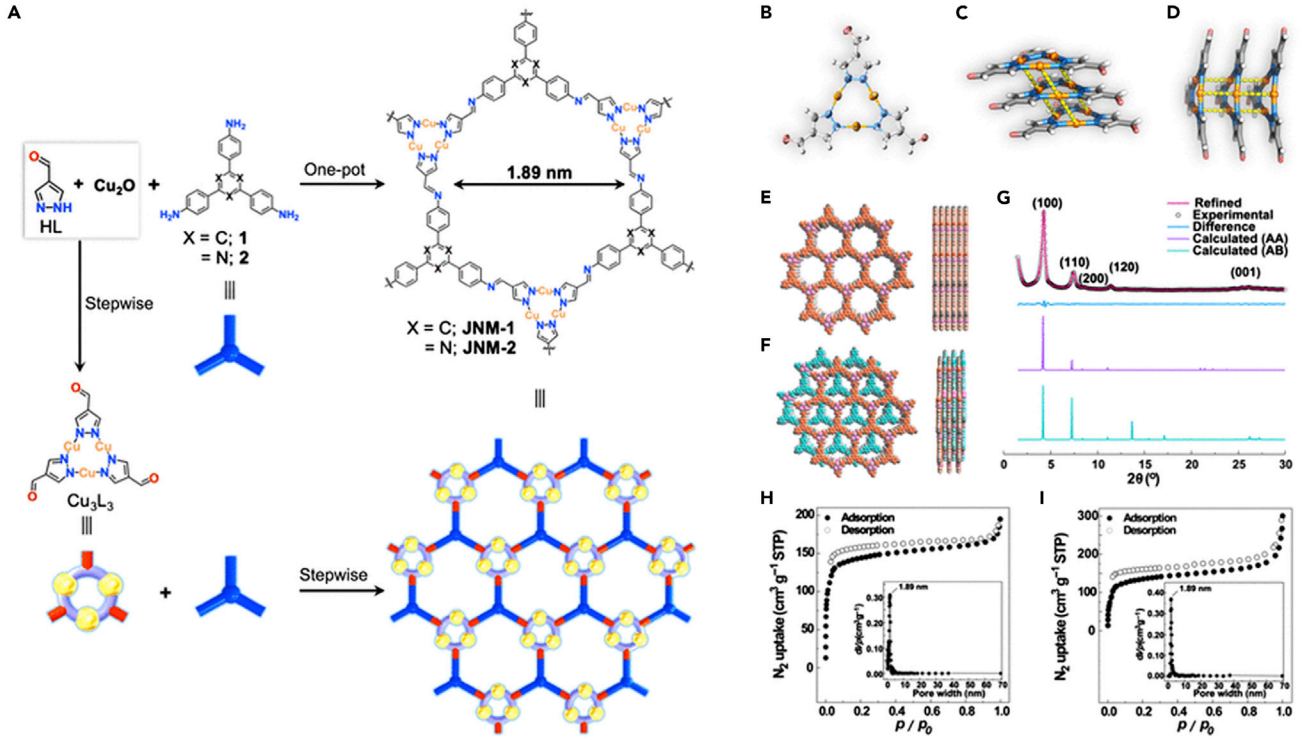

Figure 13. Preparation and characterizations of JNMs

(A) Stepwise and one-pot syntheses and structure illustration of the JNMs.

(B) ORTEP diagram at 50% level.

(C and D) (C) top view and (D) side view showing the crystal packing of Cu_3L_3 with intermolecular Cu···Cu distance of 3.74 Å.

(E and F) Structure modeling of JNM-1 exhibiting (E) AA and (F) AB packing modes shown as space-filling models.

(G) PXRD structural analysis of JNM-1.

(H and I) N_2 adsorption (filled) and desorption (open) isotherm profiles of (H) JNM-1 and (I) JNM-2 at 77 K.

From Wei et al.,[42] with permission. Copyright 2020, Chinese Chemical Society.

To summarize, the above studies show systematic synthetic pathways to construct MOF/COF composites. The basic principle for the fabrication of MOF/COF composites is the formation of covalent bond, coordination bond, hydrogen bond, and/or π-π stacking interactions between COF and MOF components. Such hybrid materials can overcome some shortcomings of individual MOFs or COFs, and create a synergistic effect to expand the application scope with optimized performance.

APPLICATION OF MOF/COF COMPOSITES

The integration of MOF and COF to form MOF/COF composites not only inherits their unique features (such as periodic network structures, high specific surface area, tunable pore sizes, and excellent chemical and thermal stability) but also creates a synergistic effect between them to afford multifunctional properties for specific applications involving adsorption and separation, heterogeneous catalysis, sensing, energy storage, and photodynamic therapy. In this section, we discuss the recent progress made by using MOF/COF composites for these applications.

Adsorption and separation

Adsorption and separation are closely related to environmental protection and energy utilization in human society. For instance, gas and liquid storage are indispensable for the widespread use of clean energy. Moreover, separation, especially for carbon dioxide (CO_2) separation from diverse mixtures including H_2, CO, N_2, and

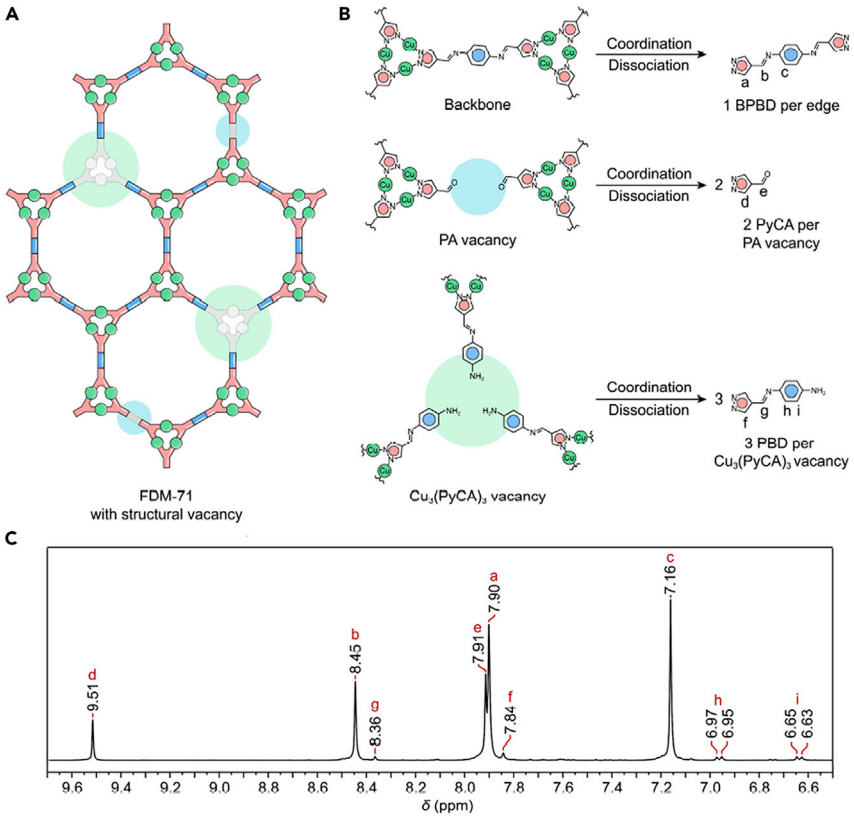

Figure 14. Identity and concentration of the vacancies in FDM-71

(A) Schematic illustration of FDM-71 with two types of structural vacancies.

(B) Identity and concentration of the vacancies could be deciphered from the obtained organic molecules after MOF digestion that dissociates only the metal-pyrazolate coordination.

(C) Solution-state ^{1}H NMR spectrum of the digested FDM-71.

From Li et al.,[38] with permission. Copyright 2019, Wiley.

CH_4, is crucial to the alleviation of the greenhouse effect. Traditional storage and separation technologies are highly energy intensive and capital intensive. By contrast, crystalline porous materials such as MOFs and COFs have been revealed as promising candidates for adsorption and separation due to their highly ordered porous structures, tunable pore sizes, and adjustable functional pore surface environment. MOF/COF hybrid materials not only maintain their original features but also provide a possible synergistic effect between COFs and MOFs for various functional applications. For instance, the C-MOF coassembly prepared by the Feng group was applied to C_2H_2, C_2H_4, C_2H_6, CH_4, CO_2, and NH_3 uptake. The uptake of these gases by C-MOF coassembly was dramatically enhanced compared with non-partitioned MOF materials.[62] Moreover, Maspoch and coworkers prepared a hierarchically porous UiO-66-NH_2@COF-TAPB-BTCA composite for water adsorption. The composite exhibits a main steep water uptake of 0.26 g g^{-1}, which is nearly 3-fold higher than that of COF-TAPB-BTCA beads (0.09 g g^{-1}) and more than 3-fold that of the physical mixture (0.07 g g^{-1}).[70] The formation of additional pores at the UiO-66-NH_2@COF-TAPB-BTCA composite interfaces can be found, which provide a synergistic increase in water uptake relative to the constituent components.

CO_2 is the most common undesired impurity in natural energy gases. Therefore, the development of efficient materials for CO_2 separation from diverse mixtures

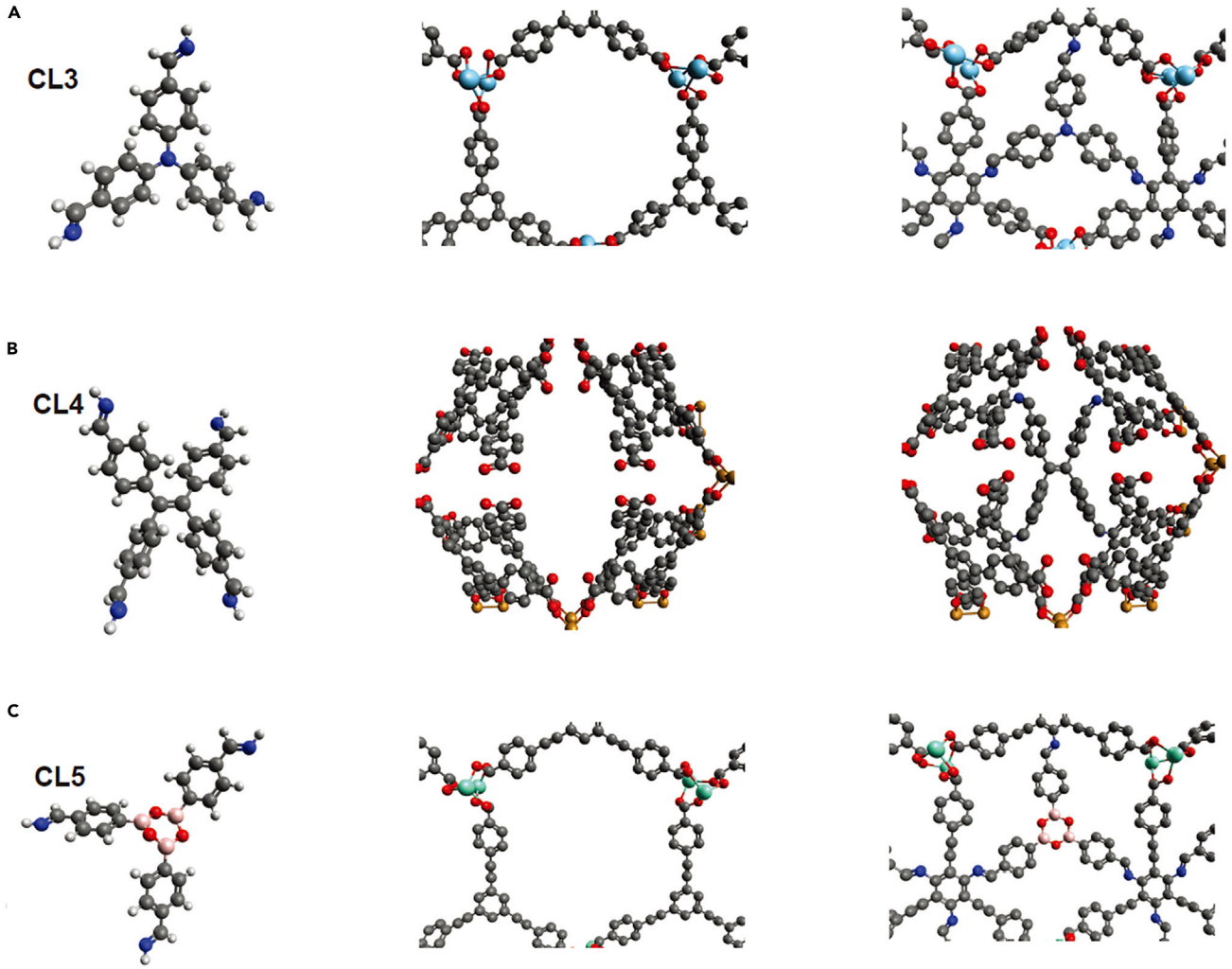

Figure 15. Three examples of COF-in-MOF

(A) The MOF "RUYVEO" can be crosslinked by using the crosslinker CL3.
(B) The MOF "QOWRAV12" can be crosslinked using crosslinker CL4.
(C) The MOF "RUYVIS" can be crosslinked by using the crosslinker CL5.
From Luo et al.,[69] with permission.

including H_2, CO, N_2, and CH_4 is a highly desired target. Recently, membrane technology has been of continuous interest for usage in gas separation due to its high energy efficiency, low operating cost, and small footprint. The balance between permeability and selectivity is an important issue in membrane separation.[47,57,58,71] Generally, due to the small sizes of gas molecules (e.g., CO_2 0.33 nm, H_2 0.29 nm), membranes with smaller pore sizes usually perform better in permselectivity, but at the same time the permeability will decrease. Given the usual monomer sizes, the pore sizes of most COFs reported are much larger than those of common gas molecules.[72] Combining COFs with larger pore sizes and MOFs with smaller pore sizes to prepare a MOF/COF composite membrane can well balance permeability and selectivity. For example, Qiu, Ben and coworkers employed [COF-300] + [Zn_2(bdc)$_2$(dabco)], [COF-300] + [ZIF-8], and [COF-300] + [UiO-66] composite membranes to separate a 1:1 binary gas mixture of H_2/CO_2. The mixture separation factors of H_2/CO_2 for the two membranes are 12.6, 13.5, and 17.2, respectively, which

surpass those for all the individual COF-300 (6.0), $Zn_2(bdc)_2(dabco)$ (7.0), ZIF-8 (9.1), and UiO-66 (9.2) membranes.[57,58] The increased gas separation selectivity of composite membranes can be attributed to the synergistic effect between COF and MOF. Different from the relatively tortuous gas diffusion paths in 3D COFs, the columnar π-arrays in 2D COFs could provide direct routes for gas diffusion, which could entail a substantial increase in gas permeability. In their later work, Ben's group prepared 2D COF-3D MOF dual-layer membranes. The resulting H_2P-DHPh COF-UiO-66 composite membrane exhibits an unprecedented H_2/CO_2 selectivity (32.9) and an ultrahigh H_2 permeability (108341.3 Barrer), which significantly outperform the present Robeson upper bound.[71] The performance of these membranes mainly relies on the interfacial interaction between the MOF and COF layers to further improve the selective separation performance of the composite membrane, Fan et al. tried to grow ZIF-67 in the confined pores of TpPa-1, which is beneficial in further reducing the pore size of the membrane and improving the precise molecular sieving properties. The selective separation performance of the composite membrane was measured following the Wicke-Kallenbach method by using single gases (H_2, CO_2, CH_4, C_3H_6, and C_3H_8) and equimolar binary mixtures (H_2/CO_2, H_2/CH_4, H_2/C_3H_6, and H_2/C_3H_8) at 298 K and 1 bar. The MOF/COF hybrid membranes exhibit an excellent hydrogen permeance of ~3,800 GPU, which is much higher than those of other tested gases. The real separation factors of the ZIF-67-in-TpPa-1 membrane for equimolar H_2/CO_2, H_2/CH_4, H_2/C_3H_6, and H_2/C_3H_8 were tested to be 34.9, 33.3, 110.5, and 192.7, respectively, which is superior to those of pure TpPa-1 membrane and ZIF-67 membrane. It is worth noting that the separation factor of H_2/CO_2 is slightly higher than that of H_2/CH_4 despite the kinetic diameter of CO_2 (0.33 nm) being smaller than that of CH_4 (0.38 nm), which could be due to a preferential adsorption of CO_2 in the nitrogen-rich membrane (Figure 16).[59]

Apart from separation for H_2/CO_2, MOF/COF composite membranes can also effectively separate CO_2/CH_4. For example, the Zhao group prepared mixed matrix membranes (MMMs) by incorporating UiO-66-NH_2@COF-TpPa-1 into a commercially available polymer, polysulfone (PSf), and explored them for CO_2/CH_4 separation. MOF@COF-based MMMs exhibit defect-free microstructures at the polymer-filler interfaces due to the high affinity between COF and PSf. More importantly, the synergistic effect of size-selective MOFs pores and polymer chain rigidification in MMMs can allow the fast and preferential permeation of CO_2 over CH_4, resulting in 48% and 79% enhancement in CO_2 permeability and CO_2/CH_4 selectivity, respectively, in sharp contrast to the pure polymeric membrane.[47]

MOF/COF composites were also used as competitive solid-phase extractants or sorbents for treatment of various industrial pollutants. For example, Firoozi et al. prepared MOF-5/COF hybrid as a robust sorbent for simultaneous removal of auramine O (AO) and rhodamine B (RB) dyes by various non-covalent interactions (e.g., electrostatic, H-bonding, and π-π stacking). The adsorption capacity for AO and RB at pH 9.5 are 17.95 and 16.18 mg g^{-1}, respectively. The removal percentage only slightly reduces over six sorption-desorption cycles, which means the stability of the core-shell MOF-5/COF composites is much improved compared with MOF-5.[73] In the year of 2020, Li et al. prepared novel magnetic Fe_3O_4@MOF@COF composites for selective separation and preconcentration of Cu^{2+}. The adsorption capacity of the magnetic composites can reach up to 37.29 mg g^{-1}. The preconcentrated Cu^{2+} could be stripped by weak acid, which then could catalyze the reaction of TMB and H_2O_2 with the detection of UV-visible spectra. The detection limit of this novel established method is 37.6 nM. Besides, Fe_3O_4@MOF@COF showed high adsorption selectivity for Cu^{2+} in multicomponent solutions containing common

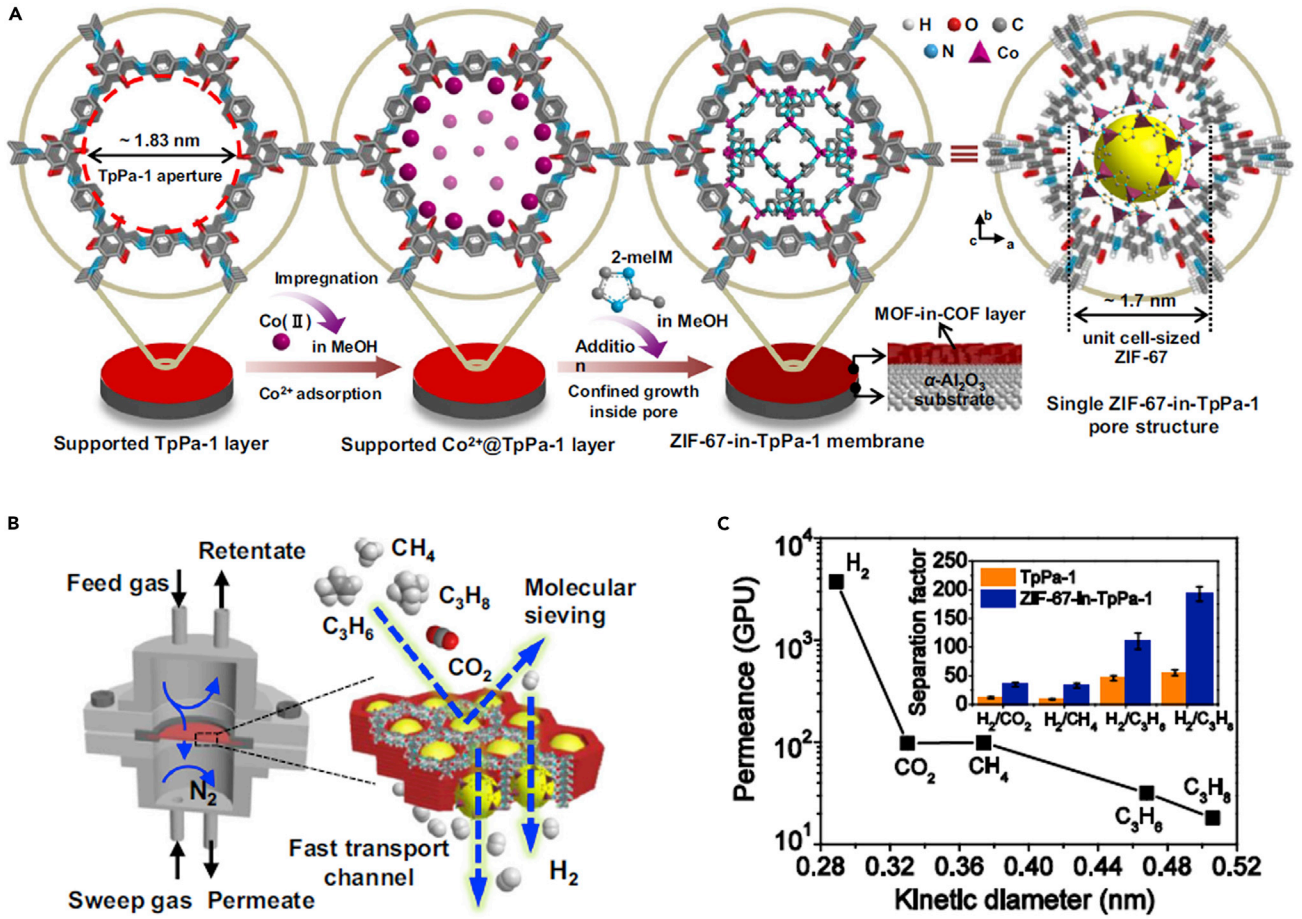

Figure 16. Preparation and separation performances of ZIF-67-in-TpPa-1

(A) Scheme depicting ZIF-67-in-TpPa-1 membrane synthesis and schematic of single pore structure.

(B) Home-made gas-permeation module and schematic illustrating gas transport through ZIF-67-in-TpPa-1 membrane.

(C) Single-gas permeances of ZIF-67-in-TpPa-1 membrane. The inset shows the mixed-gas-separation factor of ZIF-67-in-TpPa-1 membrane and TpPa-1 membrane for H_2 over other gases.

From Fan et al.,[59] with permission. Copyright 2021, Springer Nature.

monovalent and divalent competing ions.[74] In addition to the above examples, the MOF/COF composites have also been used as solid-phase sorbents for sulfonamides, sedatives, among others, providing an attractive platform for the concentration and detection of pollutants in practical samples.[75–77]

Optics and sensing

Detection of toxic, hazardous, or valuable chemical species is extremely important to maintain human health and avoid the recent threat from environmental pollution. Therefore, the development of advanced sensor materials and effective detection methods for monitoring these chemicals are highly necessary. Thanks their structural and compositional diversity, MOF/COF hybrid materials have shown great potential in sensing. For instance, Zhou et al. reported a series of Ce-MOF@COF hybrids, which were employed to detect trace oxytetracycline (OTC) through the electrochemical impedance spectroscopy (EIS) technique. The results show that Ce-MOF@-COF exhibits an ultra-low limit of detection at 17.4 fg mL^{-1} with high selectivity, good stability, and reproducibility.[53] Moreover, they also synthesized a new porous Co-MOF@TPN-COF hybrid material, which was used to detect ampicillin by the EIS

technique. The Co-MOF@TPN-COF-based aptasensor exhibits an extremely low detection limit of 0.217 fg mL^{-1} within the concentration range of 0.001 to 2,000 pg mL^{-1}. Given the high specificity of the aptamer, the proposed aptasensor also exhibits excellent selectivity along with good reproducibility, high stability, and acceptable regenerability.[53]

Facile and fast detection of antigen galectin-3 (GL-3) is desirable for clinical applications in association with heart failure risk and chronic heart failure. In 2020, Yola and Atar developed a novel sensitive amperometric method for antigen GL-3 detection based on g-C_3N_4@Au NPs and Ti-MOF@COF composites. The g-C_3N_4@Au NPs in the composites can act as the sensor platform for their rich binding sites and efficient surface conductivity while Ti-MOF@COF can act as signal amplifier due to the porous structures and stable antigen-antibody interactions. The immunosensor demonstrates a wide linearity range (0.0001–20.0 ng mL^{-1}) with a detection limit of 0.025 pg mL^{-1}, which provides an alternative tool for clinical diagnosis.[78] Although the integration of COFs and MOFs can improve the stability of MOFs to some extent, the poor electrical properties and slow carrier mobility of MOFs limit the further application of MOF/COF composites in the field of electrochemical detection. To promote the free transfer of electrons in MOF/COF composites, Zhang et al. tried to prepare a novel core-shell heterostructure by assembling well-arranged COFs on MOF-derived graphitic carbon (MOF-GC). Starting from ZIF-67, the preparation of MOF-GC undergoes two steps: (1) etching of preformed ZIF-67 with L-glutamic acid to create more pores and interface sites for COF growth; (2) thermally carbonizing the etched ZIF-67 under inert atmosphere for MOF-GC transformation. The core/shell ratio of MOF-GC@COF heterostructures can be adjusted by changing the concentration of the COF monomers from 0.002 mM to 0.05 mM, and the resulting heterostructures are named MOF-GC@$COF_{0.002}$, MOF-GC@$COF_{0.01}$, and MOF-GC@$COF_{0.05}$, respectively. Given that abundant –NH– are present in the heterostructures, the MOF-GC@COFs are expected to show high selectivity toward HCHO molecules. The HCHO response experiments show that the frequency shifts (Δf) are enhanced with increased concentration of HCHO within the range of 1–4 ppm. The average detection sensitivities of the three MOF-GC@COFs are 102.5, 151.8, and 131.3 Hz ppm^{-1}, respectively. The sensing of HCHO by MOF-GC@COF follows the pseudo-first-order kinetic model. The rapid sensing dynamics and superior HCHO sensing sensitivity over HCOOH, H_2O, NH_3, and Et_3N make MOF-GC@COF one of the best candidates for HCHO sensing (Figure 17).[79]

Besides the aforementioned electrochemical sensors, fluorescence-based sensors have gained much attention over the past decade. The luminescence of MOFs and COFs can be tuned through the alteration of metal nodes, organic ligands, and guest molecules, which offer excellent fluorescence response in analysis. For example, Yin and coworkers reported that limited COF layers on the UiO-66-NH_2 core can eliminate aggregation-caused quenching and improve the emission of COFs. When phosphate ion is added into the UiO@COF composites, the emission from UiO-66-NH_2 is enhanced while that from the COFs keeps stable. However, when ATP is added, the emission from UiO-66-NH_2 and the enol form of the COF is improved, but that from the keto state of the COF remains stable. The multiemission not only realizes ratiometric fluorescence sensing and visible detection of phosphate ions and ATP, but also provides an optional approach to the design and synthesis of other sensors (Figure 18).[80]

Catalysis

MOFs for catalysis were first reported before 2000, and COFs for catalyzing organic coupling reaction were first reported after 2011.[1] Since then, these two famous

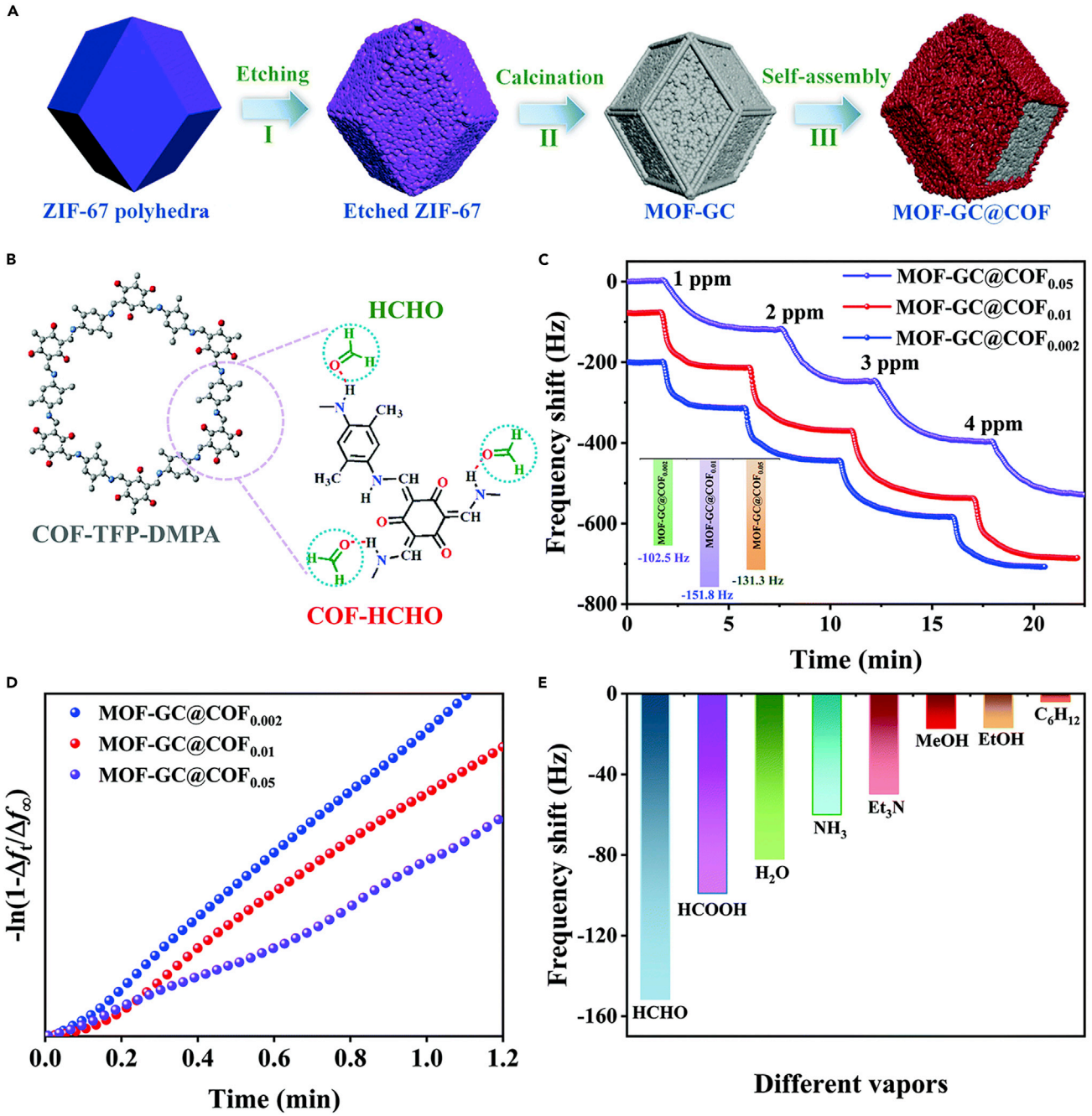

Figure 17. Preparation and catalytic performances of MOF-GC@COFs

(A) Schematic representation of the formation process of MOF-GC@COF heterostructure.

(B) Schematic showing the hydrogen-bonding interaction between COF and HCHO.

(C) Real-time dynamic frequency shift curves of MOF-GC@COFs.

(D) Graphs of pseudo-first-order kinetic model for the adsorption uptake of HCHO.

(E) Summary of frequency shifts caused by the exposure to different vapors.

From Zhang et al.,[79] with permission. Copyright 2020, Royal Society of Chemistry.

cousin frameworks have shone in the field of catalysis, from simple organic coupling reactions to asymmetric catalysis, photocatalysis, and electrocatalysis.[1,14,19,81–99] Compared with the well-developed MOF and/or COF catalysis, the development

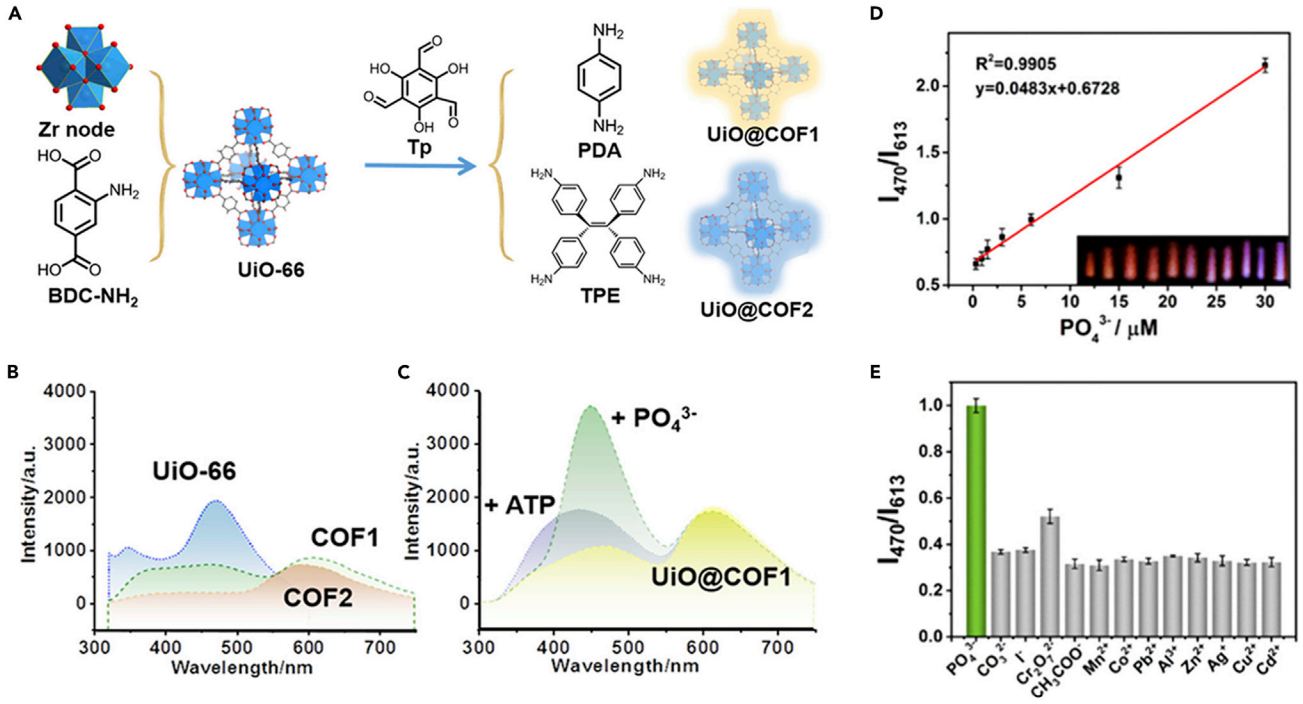

Figure 18. Design and performance of UiO@COF1 and UiO@COF2 as sensors

(A) Design of UiO@COF1 and UiO@COF2.

(B) Emission profiles of UiO-66, COF1, and COF2.

(C) Emission profiles of UiO@COF1 before and after the addition of PO_4^{3-} and ATP.

(D) Plot of the intensity ratio of I_{470}/I_{613} versus PO_4^{3-} concentration.

(E) Luminescence ratio of I_{470}/I_{613} from the responses of UiO@COF1 in the presence of PO_4^{3-} or interference ions.

From Wang et al.,[80] with permission. Copyright 2020, American Chemical Society.

of MOF/COF composite-based catalysis has just begun. In this section, we briefly introduce the latest progress in MOF/COF composites in catalysis.

Single-component MOF/COF

In 2016, Nguyen et al. prepared the first C-MOF, termed MOF-901, by combining the chemistry of MOFs and COFs. Based on titanium hexameric cluster and high conjugation system of 1,4-dialdehyde linker, MOF-901 demonstrates high performance in photocatalytic polymerization of methyl methacrylate (MMA) under visible-light irradiation. The resulting polyMMA product was obtained with large molecular weight (26,850 g mol^{-1}) and low polydispersity index (PDI) value (1.6), which is much superior to that of the control experiments given by commercial P-25 TiO_2, MIL-125-NH_2, and UiO-66-NH_2.[60] The same group further tried to engineer the optical absorption features of the resulting stable C-MOFs. In their later work, they used 4,4′-biphenyldicarboxaldehyde as the linear linker instead of 1,4-dialdehyde to form MOF-902. The longer benzene linkers promise a higher conjugation backbone in MOF-902, which is beneficial to the visible-light absorption in long-wavelength region and also to stabilization of the free radicals during the photocatalytic polymerization process. The molecular weight and PDI value of resulting polyMMA product produced by MOF-902 is 31,465 g mol^{-1} and 1.11, respectively, the former of which obviously exceeds that of MOF-901.[61] In addition to titanium-oxo clusters, the combination of polyoxometalates (POMs) and organic linkers can also provide an effective way to prepare charming photocatalysts.[64,66] For example, Ma et al. have constructed three isostructural Anderson POM-based COFs through imine condensation of NH_2-[MMo_6]-NH_2 (M = Fe, Co, Mn) and tetrahedral tetrakis(4-

formylphenyl)silicon. The incorporation of POMs into the backbones of C-MOF frameworks can enrich dye molecules and also expose more active sites, effectively increasing their photocatalytic performance for the degradation of RhB and methyl blue (MB). The M in [MMo_6] center can greatly affect the photocatalytic activity of M-Anderson-COFs. Upon irradiation for half an hour, 87.3% of the RhB was degraded using Mn-Anderson-COF, compared with 76.3% for Co-Anderson-COF and 46.0% for Fe-Anderson-COF. For photodegradation efficiencies of MB, the degradation efficiency sequence is also Mn > Co > Fe. The active species involved in the photodegradation process contain hydroxyl radicals, superoxide radical anions, holes, and singlet oxygen. The catalytic activities of the mentioned M-Anderson-COFs for oxidation of organic sulfides have also been explored. However, the catalytic activities of these three M-Anderson-COFs were almost the same.[64] Zhao et al. have also fabricated POM-based open frameworks (named NKPOM-OFs) for biomimetic catalysis. The abundant Mo=O groups in POM structures can mimic the active center of sulfite oxidase, which promises POM-based COFs great potential in biomimetic catalysis of sulfite. The sulfite oxidase activity of NKPOM-OFs was evaluated by catalyzing the reaction of SO_3^{2-} to SO_4^{2-}. The conversion efficiency of NKPOM-OF is more than 95%, far surpassing the conversion efficiency of blank reaction (<10%). The cycling performance of NKPOM-OF is excellent and can be recycled at least five times without any loss in conversion efficiency (Figure 19).[66] Recently, Li et al. fabricated a Cu-containing C-MOF, named FDM-71, by condensation an aldehyde-functionalized trinuclear Cu complex with phenylenediamine. The redox-active Cu species in FDM-71 are capable of converting H_2O_2 to $^3O_2$, which then can be converted to $^1O_2$ in light by the same photoactive FDM-71.[38] Moreover, single-component C-MOFs, i.e., JNM-1 and JNM-2, were also used for catalyzing Pd-free Sonogashira cross-coupling reaction, with excellent performance.[42]

MOF/COF composites

Integration of MOFs and COFs is an effective strategy to construct new porous hybrid composites for advanced catalysis. In 2017, Zhang and coworkers reported the first MOF@COF core-shell hybrid materials, named NH_2-MIL-68@TPA-COF, with high crystallinity and hierarchical porosity, by integrating NH_2-MIL-68 and TPA-COF. The resulting MOF@COF composites were used as a photodegradation of Rh B under visible-light irradiation as a proof-of-concept application. The corresponding experimental results show that the photodegradation rate of NH_2-MIL-68@TPA-COF is 1.4-fold faster than that of NH_2-MIL-68.[45] Furthermore, a metal-doped core-shell MOF@COF, i.e., Pd/TiATA@LZU1, was presented by the Kim group as a novel platform for tandem light-catalyzed dehydrogenation and hydrogenation reactions. The existing LZU1 in the composites has many advantages, for example, a higher charge mobility usually exists in COFs due to the ubiquitous π arrays in contrast to that of MOFs, and the evenly distributed N atoms in LZU1 can help to anchor Pd species. The results show that the COF shell functions as an electron mediator to facilitate the electron transfer from the MOF core to metal sites. Due to the structural diversities of MOFs and COFs, this "donor-mediator-acceptor" system of metal-doped MOF@COFs can offer an optional strategy for design and preparation of other efficient MOF@COF-based photocatalysts (Figure 20).[100]

The rapid recombination rate of photoinduced carriers is one of the main issues in photocatalysis. In 2019, Lu et al. successfully fabricated a core-shell MOF/COF composite, i.e., NH_2-MIL-125@TAPB-PDA, for visible-light-driven photo-oxidation of aromatic alcohols. In the photo-oxidation process, the outer-shell COFs perform more like an appropriate light-harvesting material for visible-light absorption while the inner MOF core mainly serves as catalytic active sites. The results show that the integration of NH_2-MIL-125 and TAPB-PDA can effectively enhance the optical

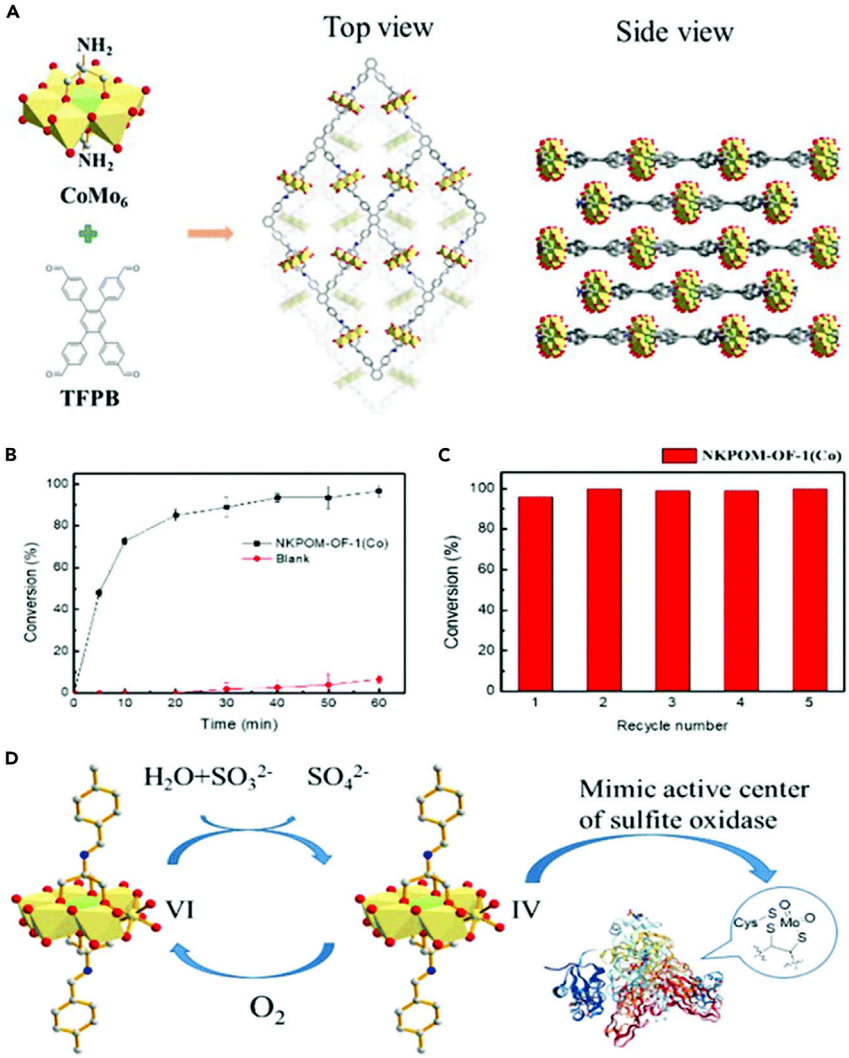

Figure 19. Preparation and catalytic performances of NKPOM-OF-1(Co)

(A) The synthetic route of NKPOM-OF-1(Co).

(B) Conversion of sulfite to sulfate catalyzed by NKPOM-OF-1(Co).

(C) Recycling experiments of NKPOM-OF-1(Co).

(D) Proposed mechanism of NKPOM-OF-1(Co) mimicking sulfite oxidase.

From Zhao et al.,[66] with permission. Copyright 2020, Royal Society of Chemistry.

absorption in the visible region and reduce the recombination rate of photogenerated carrier.[44] The same conclusion can also be drawn form a recent study by Lan and coworkers, who anchored NH_2-UiO-66 onto the surface of TpPa-1-COF to form COF@MOF composite, named NH_2-UiO-66/TpPa-1-COF. The obtained COF@MOF shows excellent photocatalytic H_2 evolution rate of 23.41 mmol g^{-1} h^{-1}, which is 20 times higher than that of the parent TpPa-1-COF.[51]

Besides photocatalysis, MOF/COF composites also exhibit superior performance in other catalytic fields. Presently, the catalytic efficiency of MOFs and COFs is unsatisfactory compared with that of natural enzymes. To improve the catalytic efficiency of MOFs, Zhang et al. constructed a nature-inspired MOF@COF nanozyme as a high-efficiency peroxidase mimic. In this ingenious composite, the MOF core was designed as catalytic sites while the COF shell was designed as the binding pockets to form a tailored

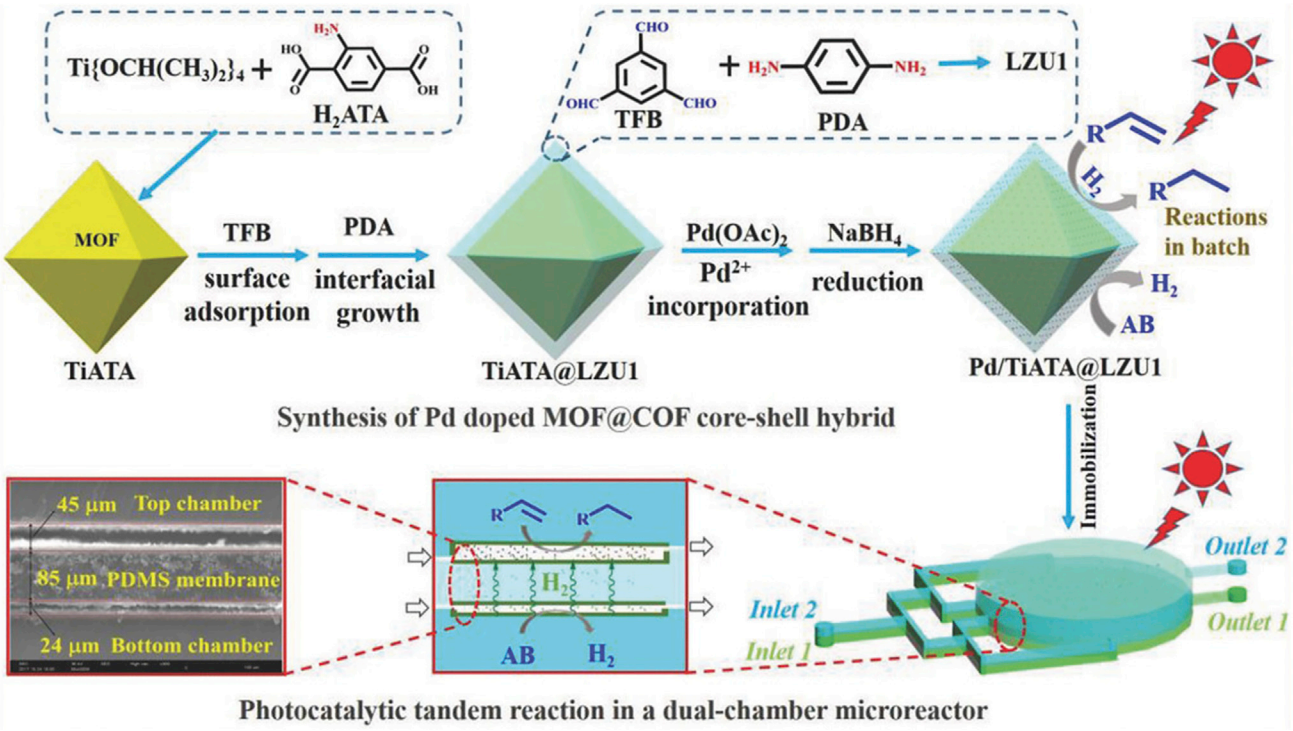

Figure 20. Preparation and photocatalytic applications of Pd-doped TiATA@LZU1

Schematic scope of the preparation of Pd-doped TiATA@LZU1 core-shell and their photocatalytic applications in batch and dual-chamber microreactor. From Sun et al.,[100] with permission. Copyright 2018, Wiley.

microenvironment around catalytic sites for substrate enrichment, organization, and activation.[101] The MOF in MOF@COF composites can also work as sacrificial templates to construct yolk-shell structure for catalytic application. For instance, Chen and coworkers developed an effective strategy to prepare hollow COF capsules for enzyme encapsulation. The yolk-shell COF/enzyme structure can greatly improve the stability and conformational freedom of enzymes inside, enhance mass transfer in the catalytic process, and ultimately boost the enzymatic activities (Figure 21).[102]

Among other examples, Gao et al. used highly stable core-shell PCN-222-Co@TpPa-1 as a bifunctional catalyst for highly efficient cascade deacetalization-Knoevenagel condensation reaction,[46] Li and coworkers fabricated a hierarchical NH_2-MIL-101(Fe)@NTU for selective styrene oxidation,[43] Zhang et al. employed MOF-derived carbon@COF heterostructures for oxygen reduction reaction,[103] and Zheng et al. used a magnetic composite Fe_3O_4@MOF_{UIO-66}@TzDa-COF with a Matryoshka structure for efficient and rapid photocatalytic degradation of Malachite green and Congo red dyes.[104] A summary of representative MOF/COF composites and their applications in catalysis is presented in Table 1.

Energy storage

The advancement of novel energy-storage devices, such as batteries and supercapacitors with superior performance, is inseparable from the innovative design and synthesis of new materials. MOFs and COFs are receiving increasing research interest in the field of energy storage. In this section, the recent development of MOF/COFs for energy storage is briefly discussed.

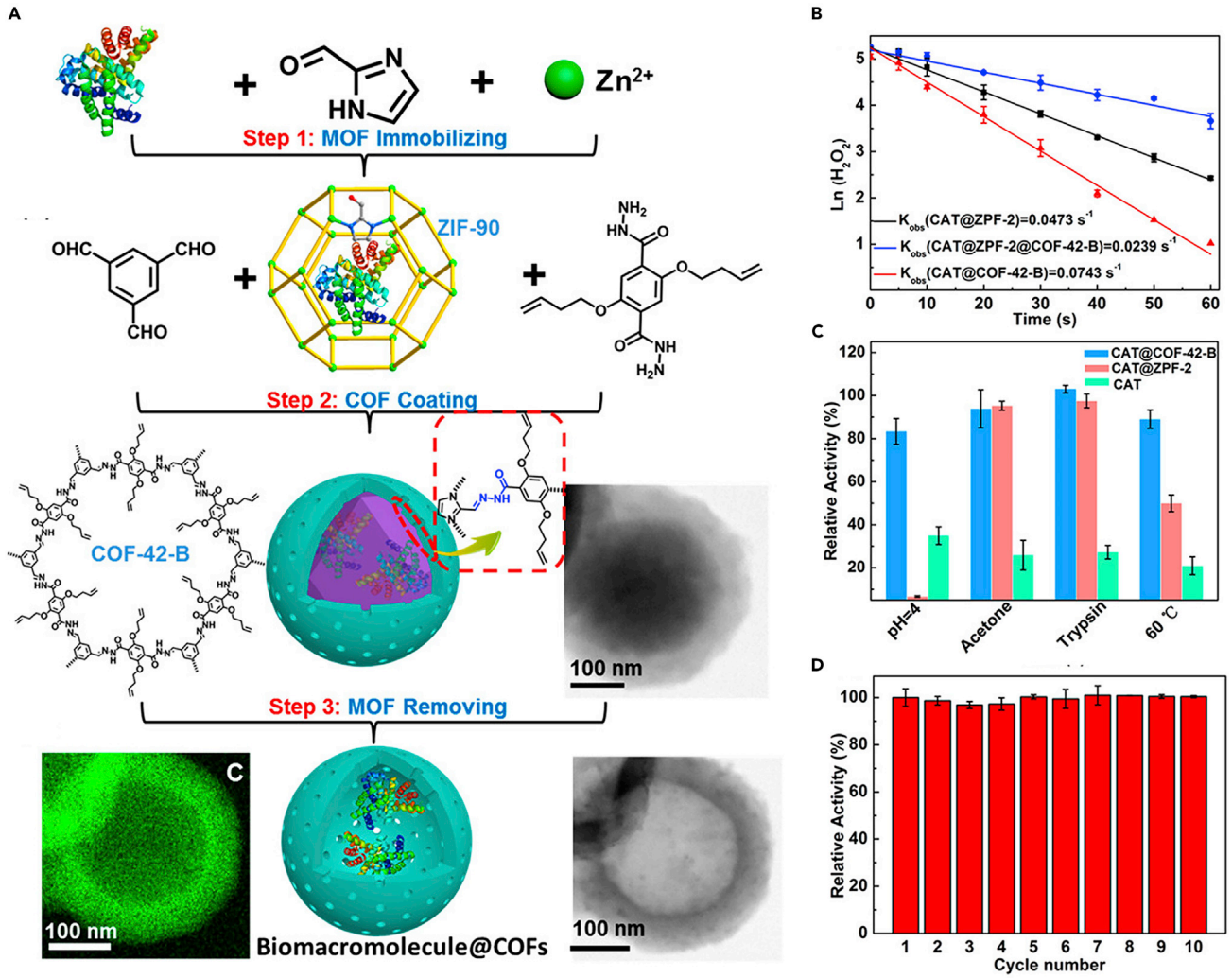

Figure 21. Preparation and catalytic performances of CAT@COF-42-B

(A) Synthetic route of biomacromolecule@COF capsules.

(B) Kinetics of degradation of H_2O_2.

(C) Activity percentage of CAT, CAT@ZPF-2, and CAT@COF-42-B after treatment under various harsh conditions.

(D) Recycling experiments of CAT@COF-42-B.

From Li et al.,[102] with permission. Copyright 2020, American Chemical Society.

Lithium batteries had made up a significant share of the consumer market because of their high energy density. Various materials have been developed for lithium storage, and related study has become a hot topic in chemistry and materials science.[108] Recently, Sun et al. used a COF@Mn-MOF based-composite for lithium storage, wherein the Mn–N coordination bond plays a vital role in the formation of interconnected composite structures. The COF@Mn-MOF capability as anode for lithium-ion batteries has proved to have a very high reversibility capacity of 1,015 mAh g^{-1} after 650 cycles, which is much superior to that of COF (126 mAh g^{-1}) and Mn-MOF (258 mAh g^{-1}). The significantly increased reversible capacities for the composites suggest an obvious synergistic effect between COF and Mn-MOF. Besides, hollow or core-shell composites of MnS@NS-C created by the sulfidation process have better properties for lithium storage than those in previous electrodes.[52] In another study, Zhuang et al. developed an N-doped porous carbon (NkPC) using a simple bottom-up strategy supported by highly

Table 1. Summary of representative MOF/COF composites and their applications in catalysis

	MOF used	COF used	Interaction	Year	Applications
MOF@COF	NH_2-MIL-68	TPA-COF	C=N	2017	photodegradation of RhB (Peng et al.[45])
	TiATA	LZU1	C=N	2018	tandem dehydrogenation and hydrogenation reactions (Sun et al.[100])
	PCN-222-Co	TpPa-1	π-π stacking	2019	cascade deacetalization-Knoevenagel condensation (Gao et al.[46])
	NH_2-MIL-125	TAPB-PDA	C=N	2019	photocatalytic oxidation of benzyl alcohol (Lu et al.[44])
	MOF-In_2S_3	FcDc-TAPT	C=N	2019	photocatalytic degradation of RhB and Cr(VI) (He et al.[48])
	NH_2-MIL-101	NTU-COF	B-O,C=N	2019	styrene oxidation (Cai et al.[43])
	NH_2-UiO-66	TFPT-DETH	C=N	2020	photocatalytic hydrogen evolution (Chen et al.[67])
	Ti-MOF	DM-LZU1	π-π stacking	2020	visible-light-promoted hydrogenation of styrene (Sun and Kim[105])
	UiO-66	TzDa-COF	π-π stacking	2020	photodegradation of anionic dyes (Zheng et al.[104])
MOF@COF-derived materials	ZIF-8	TpPa	π-π stacking	2018	catalytic reduction of 4-nitrophenol (Cui et al.[106])
	ZIF-90	COF-42	hydrazone	2020	catalyze the breakdown of hydrogen peroxide (Li et al.[102])
	ZIF-67	DAAQ-TFP	π-π stacking	2020	oxygen reduction reaction (Zhang et al.[103])
COF@MOF	NH_2-UiO-66	TpPa-1	C=N	2018	photocatalytic H_2 evolution (Zhang et al.[51])
MOF + COF	Ti-MOFs	CTF-1	amido bond	2018	visible-light-driven photocatalytic H_2 evolution (Li et al.[55])
	NH_2-MIL-125	TTB-TTA	C=N	2019	photocatalytic degradation of MO (He et al.[56])
	MIL-101-NH_2	TpMA	C=N	2019	degradation of bisphenol A (Lv et al.[107])
C-MOF	MOF-901, MOF-902			2016	photocatalyzed polymerization of methyl methacrylate (Nguyen et al.[60,61])
	M-Anderson-COFs			2020	photodegradation of RhB and MB (Ma et al.[64])
	JNM-1,JNM-2			2020	Sonogashira cross-coupling (Wei et al.[42])
	FDM-71			2020	ROS generator (Li et al.[38])
	NKPOM-OF-1(Co)			2020	sulfite oxidase (Zhao et al.[66])

dispersed Co_3O_4. In this strategy, ZIF-67 nanoparticles were first grown on a COF modified with benzoic acid (BFC) as a linker. This composite is used for two applications. The results of using this composite for electrocatalytic oxygen production (OER) reaction have shown excellent catalytic activity, and Co_3O_4/NPC-2 is entirely superior to Co_3O_4, COF, and BFC. Moreover, the use of this composite as lithium storage (used as lithium-ion battery anode) shows high reversible capacity and excellent cycling stability.[109] The C-MOF hybridizations can also be used for solid-state electrolytes in lithium batteries. In 2019, Yaghi and coworkers reported an intrinsically anionic POM-based C-MOF, termed MOF-688, with tetrabutylammonium cations as charge-balance species. After Li^+ exchange, the resulting MOF-688 shows a much higher ionic conductivity (3.4×10^{-4} S cm^{-1} at 20°C, 4.6×10^{-4} S cm^{-1} at 30°C) than other reported materials without external lithium electrolyte.[63] Later, the Fang group also employed two POM-based C-MOFs, i.e., JUC-525 and JUC-526, as anode materials for lithium-ion batteries. The electrochemical study reveals that both JUC-525 and JUC-526 displayed high

reversible capacity (as high as 550 mAh g^{-1}), rate performance, and cycling stability (up to 500 cycles), which is superior to that of NH_2-POM-NH_2, COF-300 and most POM-based MOFs.[65]

Recently, MOF@COF composites have also been used for the fabrication of a high-performance supercapacitor. It is worth pointing out that most of the COFs in MOF@COF are linked by C=N linkage, which is mainly due to the good dynamic covalent nature of C=N. In the work reported by Peng et al., a quinoline-linked aza-MOFs@COF composite was successfully synthesized with extended *p*-delocalization by post-synthetic modification of MOF@COF-LZU1 using aza-Diels-Alder cycloaddition reaction. The obtained aza-MOFs@COF is exploited as electrodes in symmetric solid-state supercapacitors. The areal capacitance and stack capacitance of aza-MOFs@COF are 20.35 $mFcm_{areal}^{-2}$ and 1.16 Fcm_{stack}^{-3}, respectively, much higher than those of UiO-66-NH_2 (7.89 $mFcm_{areal}^{-2}$ and 0.45 Fcm_{stack}^{-3}) and MOF@-COF-LZU1 (9.56 $mFcm_{areal}^{-2}$ and 0.55 Fcm_{stack}^{-3}).[50] The proposed post-synthetic modification methods can also be adopted for rational design and fabrication of other eye-catching materials in energy storage.

Photodynamic therapy

Photodynamic therapy (PDT) has attracted widespread scientific attention due to its low invasive nature and low collateral damage in healthy tissues, unlike conventional therapies. A photosensitizer (PSS) under irradiation can produce a sequence of complex photochemical and photobiological reactions to induce the apoptosis or necrosis of cancer cells by producing highly cytotoxic reactive oxygen species (ROS), in particular singlet oxygen $^1O_2$. However, the hypoxic tumor microenvironment usually lowers the therapeutic effect.[110] Therefore, it is still desirable to design and construct efficient PSS-based nanosystems for subsequent clinical translation. In 2017, Zheng and coworkers reported the use of UiO-AM@H_2P-POP composites for photodynamic therapy applications. The results of cell imaging confirmed that the composite could be effectively internalized by cancer cells. In addition, the nanocomposites displayed high phototoxicities against human hepatocellular carcinoma (HepG2) and HeLa cells under light irradiation with certain intensity while no obvious cellular death was observed in darkness.[111] This research team, in another study, used a UiO-type MOF (Hf-UiO-AM) composite, coated with a porphyrin-based COF and coated with polyethylene glycol, to kill cancer cells by producing $^1O_2$. A laser with a visible wavelength was used to excite the composite to produce $^1O_2$ that may have been caused by the presence of hafnium in the composite. The interface-based design in this study presents a feasible approach to control and improve the photochemical properties of porous materials and other nanocomplexes.[112]

CONCLUSIONS AND PERSPECTIVES

The development of MOFs and COFs has been in full swing for decades alongside their respective trajectories. Although we can obtain various MOFs or COFs with different structures by changing synthetic parameters, the synthesis of new MOF or COF structures with currently established methods may become more challenging due to the difficulties in monomer synthesis and the constraints of linkage types. The integration of MOFs and COFs into corresponding composites provides great opportunities and greatly enriches the structures and applications of these established crystalline porous frameworks.

Compared with their parent MOFs and COFs, the emergence of MOF/COF hybrid materials has just begun and is still in the nascent stage of development. Although

the existing results have shown that the performance of most hybrid materials are improved compared with the single MOFs or COFs, the potential of these hybridizations is far from being fully tapped. In terms of synthesis, due to the difficulties in crystallization the linkages of almost all COFs in MOF/COF composites are limited to C=N and B–O thus far. The good dynamic covalent nature of C=N and B–O facilitates the crystallization of COFs but will also bring about stability issues, limiting their applications under harsh conditions. It is worth noting that the synthetic systems for MOF/COF composites are much more complicated than that of "pure" COFs. Therefore, more efforts should be taken to obtain highly stable COFs with good morphology and size control in these hybrid architectures. In terms of structures, the distributions of MOFs or COFs are relatively disordered in currently reported MOF/COF composites including MOF@COF, COF@MOF, and MOF + COF. Methods for fabricating more complicated MOF/COF composites, such as COF-in-MOFs (including 0D COFs in MOFs, 2D COFs in MOFs, or 3D COFs in MOFs, as shown in Figure 2) should be further developed. Theoretically speaking, the layered or porous structures of MOFs or COFs can provide ordered confined spaces for the fabrication of fine hierarchical structures with controlled distributions. The resulting hierarchically porous structures in mesoscopic uniform distribution and related surface/interface behavior, as well as their impact on adsorption/desorption and diffusion, are closely correlated with the properties. Therefore, they will give rise to more opportunities for regulating structures, extending application scenarios, and improving related performances. In terms of functional applications, in most cases the performance of the composites is better than that of single MOFs or COFs. For instance, the hierarchically porous structures of MOF/COF composite membranes are able to well balance the permeability and selectivity, and the COF-coated MOF/COF composites can also make it easy to assemble them into MMMs, increasing their practicality. For photocatalysis, the integration could improve the stability of the composites and promote electron-hole separation during the catalytic process. However, most of the applications mentioned are designed and implemented only on the basis of experience with MOFs and/or COFs, and the in-depth mechanism studies are very limited. This situation raises the claim that not only the exploration of a wide range of application scenarios for MOF/COF hybrid materials is of importance to lay a foundation for their further development, but also the employment of computational chemistry and advanced characterization tools is necessary to underscore the critical roles of each component and the corresponding structure-activity relationship.

What unexpected new structures, properties, and applications can be brought by integration? Will the results of this integration in turn enlighten and promote the development of single MOFs and/or COFs? With continued efforts of scientists and the development of this MOF/COF integration field, we expect to see more rational and general approaches to manipulate the controlled synthesis of single-component C-MOF materials and also MOF/COF composites, thus leading to further application studies. We foresee that many exciting results related to the integration of MOFs and COFs will be reported in the near future.

ACKNOWLEDGMENTS

We gratefully acknowledge the financial support from the NSFC (21725101, 22161142001, 21871244, 21521001), Dalian National Laboratory Cooperation Fund, Chinese Academy of Sciences (DNL201911), and China Postdoctoral Science Foundation (2020M671906).

AUTHOR CONTRIBUTIONS

Conceptualization, M.K., V.S., and H.-L.J.; investigation, Y.L., M.K., and Y.-N.G; writing –original draft, Y.L., M.K., and Y.-N.G; writing – review & editing, Y.L., N.D., V.S., and H.-L.J.; funding acquisition, H.-L.J.; supervision, H.-L.J.

DECLARATION OF INTERESTS

The authors declare no competing interests.

REFERENCES

1. Rungtaweevoranit, B., Diercks, C.S., Kalmutzki, M.J., and Yaghi, O.M. (2017). Spiers memorial lecture: progress and prospects of reticular chemistry. Faraday Discuss. *201*, 9–45.
2. Gropp, C., Canossa, S., Wuttke, S., Gándara, F., Li, Q., Gagliardi, L., and Yaghi, O.M. (2020). Standard practices of reticular chemistry. ACS Cent. Sci. *6*, 1255–1273.
3. Zhou, H.-C.J., and Kitagawa, S. (2014). Metal-organic frameworks (MOFs). Chem. Soc. Rev. *43*, 5415–5418.
4. Li, B., Wen, H.-M., Cui, Y., Zhou, W., Qian, G., and Chen, B. (2016). Emerging multifunctional metal-organic framework materials. Adv. Mater. *28*, 8819–8860.
5. Diercks, C.S., Kalmutzki, M.J., Diercks, N.J., and Yaghi, O.M. (2018). Conceptual advances from werner complexes to metal-organic frameworks. ACS Cent. Sci. *4*, 1457–1464.
6. Zhang, X., Chen, Z., Liu, X., Hanna, S.L., Wang, X., Taheri-Ledari, R., Maleki, A., Li, P., and Farha, O.K. (2020). A historical overview of the activation and porosity of metal-organic frameworks. Chem. Soc. Rev. *49*, 7406–7427.
7. Bisbey, R.P., and Dichtel, W.R. (2017). Covalent organic frameworks as a platform for multidimensional polymerization. ACS Cent. Sci. *3*, 533–543.
8. Diercks, C.S., and Yaghi, O.M. (2017). The atom, the molecule, and the covalent organic framework. Science *355*, 923.
9. Geng, K., He, T., Liu, R., Dalapati, S., Tan, K.T., Li, Z., Tao, S., Gong, Y., Jiang, Q., and Jiang, D. (2020). Covalent organic frameworks: design, synthesis, and functions. Chem. Rev. *120*, 8814–8933.
10. Gong, Y.-N., Zhong, W., Li, Y., Qiu, Y., Zheng, L., Jiang, J., and Jiang, H.-L. (2020). Regulating photocatalysis by spin-state manipulation of cobalt in covalent organic frameworks. J. Am. Chem. Soc. *142*, 16723–16731.
11. Li, Y., Chen, W., Xing, G., Jiang, D., and Chen, L. (2020). New synthetic strategies toward covalent organic frameworks. Chem. Soc. Rev. *49*, 2852–2868.
12. Liang, R.-R., Jiang, S.-Y., R-H, A., and Zhao, X. (2020). Two-dimensional covalent organic frameworks with hierarchical porosity. Chem. Soc. Rev. *49*, 3920–3951.
13. Qian, Y., Li, D., Han, Y., and Jiang, H.-L. (2020). Photocatalytic molecular oxygen activation by regulating excitonic effects in covalent organic frameworks. J. Am. Chem. Soc. *142*, 20763–20771.
14. Jiao, L., Wang, Y., Jiang, H.-L., and Xu, Q. (2018). Metal-organic frameworks as platforms for catalytic applications. Adv. Mater. *30*, 1703663.
15. Lohse, M.S., and Bein, T. (2018). Covalent organic frameworks: structures, synthesis, and applications. Adv. Funct. Mater. *28*, 1705553.
16. Simon-Yarza, T., Mielcarek, A., Couvreur, P., and Serre, C. (2018). Nanoparticles of metal-organic frameworks: on the road to in vivo efficacy in biomedicine. Adv. Mater. *30*, 1707365.
17. Wei, P.F., Qi, M.Z., Wang, Z.P., Ding, S.Y., Yu, W., Liu, Q., Wang, L.K., Wang, H.Z., An, W.K., and Wang, W. (2018). Benzoxazole-linked ultrastable covalent organic frameworks for photocatalysis. J. Am. Chem. Soc. *140*, 4623–4631.
18. Yuan, S., Feng, L., Wang, K., Pang, J., Bosch, M., Lollar, C., Sun, Y., Qin, J., Yang, X., Zhang, P., et al. (2018). Stable metal-organic frameworks: design, synthesis, and applications. Adv. Mater. *30*, 1704303.
19. Jiao, L., Seow, J.Y.R., Skinner, W.S., Wang, Z.U., and Jiang, H.-L. (2019). Metal-organic frameworks: structures and functional applications. Mater. Today *27*, 43–68.
20. Liu, M., Guo, L., Jin, S., and Tan, B. (2019). Covalent triazine frameworks: synthesis and applications. J. Mater. Chem. A *7*, 5153–5172.
21. Chen, X., Geng, K., Liu, R., Tan, K.T., Gong, Y., Li, Z., Tao, S., Jiang, Q., and Jiang, D. (2020). Covalent organic frameworks: chemical approaches to designer structures and built-in functions. Angew. Chem. Int. Ed. *59*, 5050–5091.
22. Islamoglu, T., Chen, Z., Wasson, M.C., Buru, C.T., Kirlikovali, K.O., Afrin, U., Mian, M.R., and Farha, O.K. (2020). Metal-organic frameworks against toxic chemicals. Chem. Rev. *120*, 8130–8160.
23. Kuc, A., Springer, M.A., Batra, K., Juarez-Mosqueda, R., Wöll, C., and Heine, T. (2020). Proximity effect in crystalline framework materials: stacking-induced functionality in MOFs and COFs. Adv. Funct. Mater. *30*, 1908004.
24. Li, H.-Y., Zhao, S.-N., Zang, S.-Q., and Li, J. (2020). Functional metal-organic frameworks as effective sensors of gases and volatile compounds. Chem. Soc. Rev. *49*, 6364–6401.
25. Li, J., Jing, X., Li, Q., Li, S., Gao, X., Feng, X., and Wang, B. (2020). Bulk COFs and COF nanosheets for electrochemical energy storage and conversion. Chem. Soc. Rev. *49*, 3565–3604.
26. Li, W.-H., Deng, W.-H., Wang, G.-E., and Xu, G. (2020). Conductive MOFs. EnergyChem *2*, 100029.
27. Li, X., Cai, S., Sun, B., Yang, C., Zhang, J., and Liu, Y. (2020). Chemically robust covalent organic frameworks: progress and perspective. Matter *3*, 1507–1540.
28. Zhang, X., Wang, B., Alsalme, A., Xiang, S., Zhang, Z., and Chen, B. (2020). Design and applications of water-stable metal-organic frameworks: status and challenges. Coord. Chem. Rev. *423*, 213507.
29. Chen, L., and Xu, Q. (2019). Metal-organic framework composites for catalysis. Matter *1*, 57–89.
30. Furukawa, H., Cordova, K.E., O'Keeffe, M., and Yaghi, O.M. (2013). The chemistry and applications of metal-organic frameworks. Science *341*, 1230444.
31. Ding, M., Cai, X., and Jiang, H.-L. (2019). Improving MOF stability: approaches and applications. Chem. Sci. *10*, 10209–10230.
32. Gropp, C., Ma, T., Hanikel, N., and Yaghi, O.M. (2020). Design of higher valency in covalent organic frameworks. Science *370*, eabd6406.
33. Lyu, H., Ji, Z., Wuttke, S., and Yaghi, O.M. (2020). Digital reticular chemistry. Chem *6*, 2219–2241.
34. Shan, Y., Chen, L., Pang, H., and Xu, Q. (2020). Metal-organic framework-based hybrid frameworks. Small Structures *2*, 2000078.
35. Wu, M.-X., Wang, Y., Zhou, G., and Liu, X. (2020). Core-shell MOFs@MOFs: diverse designability and enhanced selectivity. ACS Appl. Mater. Interfaces *12*, 54285–54305.
36. Wu, M.-X., Wang, Y., Zhou, G., and Liu, X. (2021). Sparks from different worlds: collaboration of MOFs and COFs. Coord. Chem. Rev. *430*, 213735.
37. Dong, J., Han, X., Liu, Y., Li, H., and Cui, Y. (2020). Metal-covalent organic frameworks (MCOFs): A bridge between metal-organic frameworks and covalent organic frameworks. Angew. Chem. Int. Ed. *59*, 13722–13733.
38. Li, X., Wang, J., Xue, F., Wu, Y., Xu, H., Yi, T., and Li, Q. (2020). An imine-linked metal-organic framework as a reactive oxygen

species generator. Angew. Chem. Int. Ed. *60*, 2534–2540.

39. Hosono, N., Mochizuki, S., Hayashi, Y., and Uemura, T. (2020). Unimolecularly thick monosheets of vinyl polymers fabricated in metal-organic frameworks. Nat. Commun. *11*, 3573.

40. Lin, S., Diercks, C.S., Zhang, Y.-B., Kornienko, N., Nichols, E.M., Zhao, Y., Paris, A.R., Kim, D., Yang, P., Yaghi, O.M., and Chang, C.J. (2015). Covalent organic frameworks comprising cobalt porphyrins for catalytic CO_2 reduction in water. Science *349*, 1208–1213.

41. Liu, Y., Ma, Y., Zhao, Y., Sun, X., Gandara, F., Furukawa, H., Liu, Z., Zhu, H., Zhu, C., Suenaga, K., et al. (2016). Weaving of organic threads into a crystalline covalent organic framework. Science *351*, 365–369.

42. Wei, R.-J., Zhou, H.-G., Zhang, Z.-Y., Ning, G.-H., and Li, D. (2020). Copper (I)-organic frameworks for catalysis: networking metal clusters with dynamic covalent chemistry. CCS Chem. *2*, 2045–2053.

43. Cai, M., Li, Y., Liu, Q., Xue, Z., Wang, H., Fan, Y., Zhu, K., Ke, Z., Su, C.Y., and Li, G. (2019). One-step construction of hydrophobic MOFs@COFs core-shell composites for heterogeneous selective catalysis. Adv. Sci. *6*, 1802365.

44. Lu, G., Huang, X., Li, Y., Zhao, G., Pang, G., and Wang, G. (2020). Covalently integrated core-shell MOF@COF hybrids as efficient visible-light-driven photocatalysts for selective oxidation of alcohols. J. Energy Chem. *43*, 8–15.

45. Peng, Y., Zhao, M., Chen, B., Zhang, Z., Huang, Y., Dai, F., Lai, Z., Cui, X., Tan, C., and Zhang, H. (2017). Hybridization of MOFs and COFs: a new strategy for construction of MOF@COF core-shell hybrid materials. Adv. Mater. *30*, 1705454.

46. Gao, M.-L., Qi, M.-H., Liu, L., and Han, Z.-B. (2019). An exceptionally stable core-shell MOF/COF bifunctional catalyst for a highly efficient cascade deacetalization-Knoevenagel condensation reaction. Chem. Commun. *55*, 6377–6380.

47. Cheng, Y., Ying, Y., Zhai, L., Liu, G., Dong, J., Wang, Y., Christopher, M.P., Long, S., Wang, Y., and Zhao, D. (2019). Mixed matrix membranes containing MOF@COF hybrid fillers for efficient CO_2/CH_4 separation. J. Membr. Sci. *573*, 97–106.

48. He, R., Xue, K., Wang, J., Yang, T., Sun, R., Wang, L., Yu, X., Omeoga, U., Wang, W., Yang, T., et al. (2019). Design and synthesis of La^{3+}-, Sb^{3+}-doped MOF-In_2S_3@FcDc-TAPT COFs hybrid materials with enhanced photocatalytic activity. J. Mater. Sci. *54*, 14690–14706.

49. Yao, Y., Zhang, R., Liu, T., Yu, H., and Lu, G. (2019). Controlled synthesis of core-shell composites with uniform shells of a covalent organic framework. Inorg. Chem. Commun. *101*, 160–163.

50. Peng, H., Raya, J., Richard, F., Baaziz, W., Ersen, O., Ciesielski, A., and Samorì, P. (2020). Synthesis of robust MOFs@COFs porous hybrid materials via an aza-Diels-Alder reaction: towards high-performance supercapacitor materials. Angew. Chem. Int. Ed. *59*, 19602–19609.

51. Zhang, F.-M., Sheng, J.-L., Yang, Z.-D., Sun, X.-J., Tang, H.-L., Lu, M., Dong, H., Shen, F.-C., Liu, J., and Lan, Y.-Q. (2018). Rational design of MOF/COF hybrid materials for photocatalytic H_2 evolution in the presence of sacrificial electron donors. Angew. Chem. Int. Ed. *57*, 12106–12110.

52. Sun, W., Tang, X., Yang, Q., Xu, Y., Wu, F., Guo, S., Zhang, Y., Wu, M., and Wang, Y. (2019). Coordination-induced interlinked covalent-and metal-organic-framework hybrids for enhanced lithium storage. Adv. Mater. *31*, 1903176.

53. Zhou, N., Ma, Y., Hu, B., He, L., Wang, S., Zhang, Z., and Lu, S. (2019). Construction of Ce-MOF@COF hybrid nanostructure: label-free aptasensor for the ultrasensitive detection of oxytetracycline residues in aqueous solution environments. Biosens. Bioelectron. *127*, 92–100.

54. Feng, L., Wang, K.-Y., Lv, X.-L., Yan, T.-H., Li, J.-R., and Zhou, H.-C. (2020). Modular total synthesis in reticular chemistry. J. Am. Chem. Soc. *142*, 3069–3076.

55. Li, F., Wang, D., Xing, Q.-J., Zhou, G., Liu, S.-S., Li, Y., Zheng, L.-L., Ye, P., and Zou, J.-P. (2019). Design and syntheses of MOF/COF hybrid materials via postsynthetic covalent modification: an efficient strategy to boost the visible-light-driven photocatalytic performance. Appl. Catal. B *243*, 621–628.

56. He, S., Rong, Q., Niu, H., and Cai, Y. (2019). Platform for molecular-material dual regulation: a direct Z-scheme MOF/COF heterojunction with enhanced visible-light photocatalytic activity. Appl. Catal. B *247*, 49–56.

57. Fu, J., Das, S., Xing, G., Ben, T., Valtchev, V., and Qiu, S. (2016). Fabrication of COF-MOF composite membranes and their highly selective separation of H_2/CO_2. J. Am. Chem. Soc. *138*, 7673–7680.

58. Das, S., and Ben, T. (2018). A [COF-300]-[UiO-66] composite membrane with remarkably high permeability and H_2/CO_2 separation selectivity. Dalton Trans. *47*, 7206–7212.

59. Fan, H., Peng, M., Strauss, I., Mundstock, A., Meng, H., and Caro, J. (2021). MOF-in-COF molecular sieving membrane for selective hydrogen separation. Nat. Commun. *12*, 38.

60. Nguyen, H.L., Gándara, F., Furukawa, H., Doan, T.L.H., Cordova, K.E., and Yaghi, O.M. (2016). A titanium-organic framework as an exemplar of combining the chemistry of metal-and covalent-organic frameworks. J. Am. Chem. Soc. *138*, 4330–4333.

61. Nguyen, H.L., Vu, T.T., Le, D., Doan, T.L.H., Nguyen, V.Q., and Phan, N.T.S. (2016). A Titanium-organic framework: engineering of the band-gap energy for photocatalytic property enhancement. ACS Catal. *7*, 338–342.

62. Wang, Y., Zhao, X., Yang, H., Bu, X., Wang, Y., Jia, X., Li, J., and Feng, P. (2019). A tale of two trimers from two different worlds: a COF-inspired synthetic strategy for pore-space partitioning of MOFs. Angew. Chem. Int. Ed. *58*, 6316–6320.

63. Xu, W., Pei, X., Diercks, C.S., Lyu, H., Ji, Z., and Yaghi, O.M. (2019). A metal-organic framework of organic vertices and polyoxometalate linkers as a solid-state electrolyte. J. Am. Chem. Soc. *141*, 17522–17526.

64. Ma, R., Liu, N., Lin, T.-T., Zhao, T., Huang, S.-L., and Yang, G.-Y. (2020). Anderson polyoxometalate built-in covalent organic frameworks for enhancing catalytic performances. J. Mater. Chem. A *8*, 8548–8553.

65. Yu, X., Li, C., Ma, Y., Li, D., Li, H., Guan, X., Yan, Y., Valtchev, V., Qiu, S., and Fang, Q. (2020). Crystalline, porous, covalent polyoxometalate-organic frameworks for lithium-ion batteries. Microporous Mesoporous Mater. *299*, 110105.

66. Zhao, Y., Wang, Z., Gao, J., Zhao, Z., Li, X., Wang, T., Cheng, P., Ma, S., Chen, Y., and Zhang, Z. (2020). COF-inspired fabrication of two-dimensional polyoxometalate based open frameworks for biomimetic catalysis. Nanoscale *12*, 21218–21224.

67. Chen, Y., Yang, D., Shi, B., Dai, W., Ren, H., An, K., Zhou, Z., Zhao, Z., Wang, W., and Jiang, Z. (2020). In situ construction of hydrazone-linked COF-based core-shell hetero-frameworks for enhanced photocatalytic hydrogen evolution. J. Mater. Chem. A *8*, 7724–7732.

68. Ishiwata, T., Furukawa, Y., Sugikawa, K., Kokado, K., and Sada, K. (2013). Transformation of metal-organic framework to polymer gel by cross-linking the organic ligands preorganized in metal-organic framework. J. Am. Chem. Soc. *135*, 5427–5432.

69. Luo, Y., Wöll, C., Ahmad, M., Schug, A., and Tsotsalas, M. (2020). Design of metal-organic framework templated materials using high-throughput computational screening. ChemRxiv. https://doi.org/10.26434/chemrxiv.12888296.v2.

70. Garzón-Tovar, L., Pérez-Carvajal, J., Yazdi, A., Hernández-Muñoz, J., Tarazona, P., Imaz, I., Zamora, F., and Maspoch, D. (2019). A MOF@COF composite with enhanced uptake through interfacial pore generation. Angew. Chem. Int. Ed. *58*, 9512–9516.

71. Das, S., Ben, T., Qiu, S., and Valtchev, V. (2020). Two-dimensional COF-three-dimensional MOF dual-layer membranes with unprecedentedly high H_2/CO_2 selectivity and ultrahigh gas permeabilities. ACS Appl. Mater. Interfaces *12*, 52899–52907.

72. Li, Y., Wu, Q., Guo, X., Zhang, M., Chen, B., Wei, G., Li, X., Li, X., Li, S., and Ma, L. (2020). Laminated self-standing covalent organic framework membrane with uniformly distributed subnanopores for ionic and molecular sieving. Nat. Commun. *11*, 599.

73. Firoozi, M., Rafiee, Z., and Dashtian, K. (2020). New MOF/COF hybrid as a robust adsorbent for simultaneous removal of Auramine O and Rhodamine B dyes. ACS Omega *5*, 9420–9428.

74. Li, W.-T., Shi, W., Hu, Z.-J., Yang, T., Chen, M.-L., Zhao, B., and Wang, J.-H. (2020). Fabrication of magnetic Fe_3O_4@metal organic framework@covalent organic framework composite and its selective separation of trace copper. Appl. Surf. Sci. *530*, 147254.

75. Chen, Z., Yu, C., Xi, J., Tang, S., Bao, T., and Zhang, J. (2019). A hybrid material prepared by controlled growth of a covalent organic framework on amino-modified MIL-68 for pipette tip solid-phase extraction of sulfonamides prior to their determination by HPLC. Microchim. Acta *186*, 393.

76. Liu, J., Li, G., Wu, D., Yu, Y., Chen, J., and Wu, Y. (2020). Facile preparation of magnetic covalent organic framework-metal organic framework composite materials as effective adsorbents for the extraction and determination of sedatives by high-performance liquid chromatography/tandem mass spectrometry in meat samples. Rapid Commun. Mass Spectrom. *34*, e8742.

77. Yue, B., Liu, J., Li, G., and Wu, Y. (2020). Synthesis of magnetic metal organic framework/covalent organic framework hybrid materials as adsorbents for magnetic solid-phase extraction of four endocrine-disrupting chemicals from milk samples. Rapid Commun. Mass Spectrom. *34*, e8909.

78. Yola, M.L., and Atar, N. (2020). Amperometric galectin-3 immunosensor-based gold nanoparticle-functionalized graphitic carbon nitride nanosheets and core-shell Ti-MOF@COFs composites. Nanoscale *12*, 19824–19832.

79. Zhang, S., Yang, Q., Xu, X., Liu, X., Li, Q., Guo, J., Torad, N.L., Alshehri, S.M., Ahamad, T., Hossain, M.S.A., et al. (2020). Assembling well-arranged covalent organic frameworks on MOF-derived graphitic carbon for remarkable formaldehyde sensing. Nanoscale *12*, 15611–15619.

80. Wang, X.-Y., Yin, H.-Q., and Yin, X.-B. (2020). MOF@COFs with strong multiemission for differentiation and ratiometric fluorescence detection. ACS Appl. Mater. Interfaces *12*, 20973–20981.

81. Banerjee, T., Gottschling, K., Savasci, G., Ochsenfeld, C., and Lotsch, B.V. (2018). H_2 evolution with covalent organic framework photocatalysts. ACS Energy Lett. *3*, 400–409.

82. Chen, Y.-Z., Zhang, R., Jiao, L., and Jiang, H.-L. (2018). Metal-organic framework-derived porous materials for catalysis. Coord. Chem. Rev. *362*, 1–23.

83. Dhakshinamoorthy, A., Li, Z., and Garcia, H. (2018). Catalysis and photocatalysis by metal organic frameworks. Chem. Soc. Rev. *47*, 8134–8172.

84. Lin, C.Y., Zhang, D., Zhao, Z., and Xia, Z. (2018). Covalent organic framework electrocatalysts for clean energy conversion. Adv. Mater. *30*, 1703646.

85. Wang, C., An, B., and Lin, W. (2018). Metal-organic frameworks in solid-gas phase catalysis. ACS Catal. *9*, 130–146.

86. Xiao, J.-D., and Jiang, H.-L. (2018). Metal-organic frameworks for photocatalysis and photothermal catalysis. Acc. Chem. Res. *52*, 356–366.

87. Yan, Y., He, T., Zhao, B., Qi, K., Liu, H., and Xia, B.Y. (2018). Metal/covalent-organic frameworks-based electrocatalysts for water splitting. J. Mater. Chem. A *6*, 15905–15926.

88. Yang, S., Hu, W., Zhang, X., He, P., Pattengale, B., Liu, C., Cendejas, M., Hermans, I., Zhang, X., Zhang, J., and Huang, J. (2018). 2D Covalent organic frameworks as intrinsic photocatalysts for visible light driven CO_2 reduction. J. Am. Chem. Soc. *140*, 14614–14618.

89. Dhakshinamoorthy, A., Asiri, A.M., and Garcia, H. (2019). 2D Metal-organic frameworks as multifunctional materials in heterogeneous catalysis and electro/photocatalysis. Adv. Mater. *31*, 1900617.

90. Ding, M., Flaig, R.W., Jiang, H.-L., and Yaghi, O.M. (2019). Carbon capture and conversion using metal-organic frameworks and MOF-based materials. Chem. Soc. Rev. *48*, 2783–2828.

91. Jiao, L., and Jiang, H.-L. (2019). Metal-organic-framework-based single-atom catalysts for energy applications. Chem *5*, 786–804.

92. Li, D., Xu, H.-Q., Jiao, L., and Jiang, H.-L. (2019). Metal-organic frameworks for catalysis: state of the art, challenges, and opportunities. EnergyChem *1*, 100005.

93. Liu, H., and Jiang, H.-L. (2019). Solar-powered artificial photosynthesis coupled with organic synthesis. Chem *5*, 2508–2510.

94. Bavykina, A., Kolobov, N., Khan, I.S., Bau, J.A., Ramirez, A., and Gascon, J. (2020). Metal-organic frameworks in heterogeneous catalysis: recent progress, new trends, and future perspectives. Chem. Rev. *120*, 8468–8535.

95. Dhakshinamoorthy, A., Asiri, A.M., and García, H. (2020). Metal-organic frameworks as multifunctional solid catalysts. Trends Chem. *2*, 454–466.

96. Han, X., Yuan, C., Hou, B., Liu, L., Li, H., Liu, Y., and Cui, Y. (2020). Chiral covalent organic frameworks: design, synthesis and property. Chem. Soc. Rev. *49*, 6248–6272.

97. Liang, Q., Chen, J., Wang, F., and Li, Y. (2020). Transition metal-based metal-organic frameworks for oxygen evolution reaction. Coord. Chem. Rev. *424*, 213488.

98. Liu, Y., Zhou, W., Teo, W.L., Wang, K., Zhang, L., Zeng, Y., and Zhao, Y. (2020). Covalent-organic-framework-based composite materials. Chem *6*, 3172–3202.

99. Wei, Y.-S., Zhang, M., Zou, R., and Xu, Q. (2020). Metal-organic framework-based catalysts with single metal sites. Chem. Rev. *120*, 12089–12174.

100. Sun, D., Jang, S., Yim, S.-J., Ye, L., and Kim, D.-P. (2018). Metal doped core-shell metal-organic frameworks@covalent organic frameworks (MOFs@COFs) hybrids as a novel photocatalytic platform. Adv. Funct. Mater. *28*, 1707110.

101. Zhang, L., Liu, Z., Deng, Q., Sang, Y., Dong, K., Ren, J., and Qu, X. (2020). Nature-inspired construction of MOF@COF nanozyme with active sites in tailored microenvironment and pseudopodia-like surface for enhanced bacterial inhibition. Angew. Chem. Int. Ed. *60*, 3469–3474.

102. Li, M., Qiao, S., Zheng, Y., Andaloussi, Y.H., Li, X., Zhang, Z., Li, A., Cheng, P., Ma, S., and Chen, Y. (2020). Fabricating covalent organic framework capsules with commodious microenvironment for enzymes. J. Am. Chem. Soc. *142*, 6675–6681.

103. Zhang, S., Xia, W., Yang, Q., Valentino Kaneti, Y., Xu, X., Alshehri, S.M., Ahamad, T., Hossain, M.S.A., Na, J., Tang, J., and Yamauchi, Y. (2020). Core-shell motif construction: highly graphitic nitrogen-doped porous carbon electrocatalysts using MOF-derived carbon@COF heterostructures as sacrificial templates. Chem. Eng. J. *396*, 125154.

104. Zheng, M., Yao, C., and Xu, Y. (2020). Fe_3O_4 nanoparticles decorated with UIO-66 metal-organic framework particles and encapsulated in a triazine-based covalent organic framework matrix for photodegradation of anionic dyes. ACS Appl. Nano Mater. *3*, 11307–11314.

105. Sun, D., and Kim, D.-P. (2020). Hydrophobic MOFs@metal nanoparticles@COFs for interfacially confined photocatalysis with high efficiency. ACS Appl. Mater. Interfaces *12*, 20589–20595.

106. Cui, K., Zhong, W., Li, L., Zhuang, Z., Li, L., Bi, J., and Yu, Y. (2018). Well-defined metal nanoparticles@covalent organic framework yolk-shell nanocages by ZIF-8 template as catalytic nanoreactors. Small *15*, 1804419.

107. Lv, S.-W., Liu, J.-M., Li, C.-Y., Zhao, N., Wang, Z.-H., and Wang, S. (2020). Two novel MOFs@COFs hybrid-based photocatalytic platforms coupling with sulfate radical-involved advanced oxidation processes for enhanced degradation of bisphenol A. Chemosphere *243*, 125378.

108. Xu, G., Nie, P., Dou, H., Ding, B., Li, L., and Zhang, X. (2017). Exploring metal organic frameworks for energy storage in batteries and supercapacitors. Mater. Today *20*, 191–209.

109. Zhuang, G.-l., Gao, Y.-f., Zhou, X., Tao, X.-y., Luo, J.-m., Gao, Y.-j., Yan, Y.-l., Gao, P.-y., Zhong, X., and Wang, J.-g. (2017). ZIF-67/COF-derived highly dispersed Co_3O_4/N-doped porous carbon with excellent performance for oxygen evolution reaction and Li-ion batteries. Chem. Eng. J. *330*, 1255–1264.

110. Dmitriev, R.I., Borisov, S.M., Düssmann, H., Sun, S., Müller, B.J., Prehn, J., Baklaushev, V.P., Klimant, I., and Papkovsky, D.B. (2015). Versatile conjugated polymer nanoparticles for high-resolution O_2 imaging in cells and 3D tissue models. ACS Nano *9*, 5275–5288.

111. Zheng, X., Wang, L., Pei, Q., He, S., Liu, S., and Xie, Z. (2017). Metal-organic framework@porous organic polymer nanocomposite for photodynamic therapy. Chem. Mater. *29*, 2374–2381.

112. Zheng, X., Wang, L., Guan, Y., Pei, Q., Jiang, J., and Xie, Z. (2020). Integration of metal-organic framework with a photoactive porous-organic polymer for interface enhanced phototherapy. Biomaterials *235*, 119792.